Ammitocyon kainos gen. et sp. nov., a chimerical amphicyonid (Mammalia, Carnivora) from the late Miocene carnivore traps of Cerro de los Batallones (Madrid, Spain)

Jorge Morales[a], Juan Abella[b,c,*], Oscar Sanisidro[d] and Alberto Valenciano[e]

[a]Departamento de Paleobiología, Museo Nacional de Ciencias Naturales-CSIC, C/José Gutiérrez Abascal, 2, 28006 Madrid, Spain; [b]Institut Català de Paleontologia Miquel Crusafont, Edifici Institut de Ciència i Tecnologia Ambientals - Institut Català de Paleontologia (ICTA-ICP), Campus de la UAB, Carrer de les Columnes s/n, 08193, Cerdanyola del Vallès, 08193, Barcelona; [c]Instituto Nacional de Biodiversidad, Pje, Rumipamba N. 341 y Av. de los Shyris (Parque La Carolina), Quito, Ecuador; [d]Departamento de Ciencias de la Vida, GloCEE Global Change Ecology and Evolution Research Group, Universidad de Alcalá, Plaza de San Diego s/n, Alcalá de Henares, 28801 Madrid, Spain; [e]Departamento de Ciencias de la Tierra and Instituto Universitario de Investigación en Ciencias Ambientales de Aragón (IUCA), Universidad de Zaragoza, 50009 Zaragoza, Spain

(Received 18 January 2021; accepted 11 March 2021)

In the present paper, we describe the cranio-dental remains of three individuals of an Amphicyonidae previously determined as *Thaumastocyon* sp. from the late Miocene (*c*. 9 Ma) pseudokarstic site of Batallones-3. Dentognathic differences in relation to other Thaumastocyoninae enable a new taxon, *Ammitocyon kainos* gen. et sp. nov., to be

defined; it is both the most recent and the most complete member of this subfamily known in the fossil record. The results of our phylogenetic analysis demonstrate that this new form reached the maximum degree of specialization within Thaumastocyoninae, a group that includes the most hypercarnivorous Amphicyonidae species of the Miocene. The masticatory apparatus of *A. kainos* is extremely derived, with the loss of the mesial premolars (P3 / P2 and p1–p3) and the third molars (M3 / m3). The robustness of the chin and muzzle is in contrast with the slender and highly sectorial postcanine dentition (p4 / m2 and P4 / M2), features that are consistent with the values provided by the analysis of the bending resistance of the mandible performed for these specimens. All the anatomical features combined, both cranial and postcranial, reveal the complexity of the body plan of *A. kainos*. This species combines derived hypercarnivorous dentition with one of the most robust postcranial skeletons recorded for all large caniform carnivorans, outlining an enigmatic taxon that presents unique ecological adaptations.

Keywords: Carnivora; Amphicyonidae; hypercarnivory; late Miocene; Iberian Peninsula

https://zoobank.org/urn:lsid:zoobank.org:pub:

*Corresponding author. Email: juan.abella@icp.cat

Introduction

Amphicyonidae constituted one of the most important groups of caniform carnivorans for many of the Cenozoic European and North American faunas; from approximately 40 Ma until 9 Ma, when they disappear simultaneously from both continents (Hunt 1998; Werdelin & Simpson 2009). Tomiya & Tseng (2016), recently proposed a North American origin for this family, based on the significant cladogenesis experienced by the family on this continent during the Eocene. Unlike the Amphicyonidae associations of North America, the Eocene fossil record in Europe displays a lower level of diversity (Springhorn 1997). However, during the Oligocene and especially the Miocene, the European Amphicyonidae became highly diverse, presenting a wide range of both sizes and dental adaptations. Three subfamilies are commonly recognized in Europe during this period: Amphicyoninae Trouessart (1885), Haplocyoninae De Bonis (1996) and Thaumastocyoninae Hürzeler (1940). Interestingly, all three groups reached a hypercarnivorous adaptive peak at some points in their fossil records, albeit through disparate modifications of their dentition (Hunt 1998). The first one of these groups to develop a derived sectorial morphology was Haplocyoninae, which have been closely related to the North American Temnocyoninae Hunt (1998) (Ginsburg 1999; Hunt 2011). Both Haplocyoninae and Temnocyoninae show a profound modification of their dentitions, as observed in *Haplocyonoides mordax* Hürzeler (1940) and *Haplocyonoides suevicus* Peigné & Heizmann (2003), which represent the last members of Haplocyoninae in Western Europe. In these species, both molars are derived, lacking lingual cuspids. The lower carnassial only comprises a paraconid, a protoconid and a hypoconid, all of which are aligned and buccolingually compressed. Similarly, the m2 is restricted to the protoconid and the hypoconid. However, neither of these two molars shows a pronounced mesiodistal elongation characteristic of the more hypercarnivorous forms. Additionally, there is no elongation of the P4, which is still short and robust with

a very strong and lingually projected protocone. The upper molars retain an unequivocal lingual development, albeit with a narrow protocone. The buccal cusps of the M1 are low and separated from the protocone by a deep depression for the occlusion of the m1 hypoconid. Furthermore, similar to what occurs in Temnocyonine, the premolars are robust, showing no reduction in size or number. Hence, both these subfamilies developed a mixed dental pattern combining both shearing and crushing functions in a manner unique to the Carnivora (Hunt 1998, 2011). A particular case involves *Daphoenictis tedfordi* Hunt (1974), which displays a precocious hypercarnivore dentition rather different from other amphicyonids. The lower premolars are long, sharp and possess a well-developed distal and mesial accessory cusp, analogous to the premolars of the extant *Lycaon pictus*. Nonetheless, the lower and upper molar dentition is more conservative, as in Haplocyoninae, albeit more sectorial (Emry & Hunt 1985; Boardman & Hunt 2015). The last Haplocyoninae are recorded in the lower Miocene (MN 2/3), coinciding with the appearance of the first Thaumastocyoninae such as *Ysengrinia* Ginsburg, 1966, *Crassidia* Heizmann & Kordikova, 2000 or *Peignecyon* Morales, Fejfar, Heizmann, Wagner, Valenciano & Abella, 2019, forms which are still morphologically closer to the early Miocene Amphicyoninae (Morales *et al.* 2019). Amphicyoninae and Thaumastocyoninae survived into the late Miocene, but with a notable and gradual decline in diversity. Some of these latest representatives coexisted on the Iberian Peninsula, sharing an advanced hypercarnivorous dentition (Peigné *et al.* 2008; Morales *et al.* 2017, 2019). Among them is *Magericyon* Peigné, Salesa, Antón & Morales, 2008, a hypercarnivorous Amphicyoninae that appears sparsely in the fossil record during the Vallesian (Ginsburg *et al.* 1981; Peignè *et al.* 2008). The adaptations of *Magericyon* towards hypercarnivory differ from those of Haplocyoninae, not only in the reduction of the premolars but also in the transformation of the entire dentition

towards a hypercarnivorous model. This clearly indicates an Amphicyoninae origin in contraposition with Haplocyoninae hypercarnivorism derived from the more plesiomorphic taxa. Although this Amphicyoninae displays a rather derived morphology, however, there is a qualitative jump towards hypercarnivorous adaptation in the late Miocene Thaumastocyoninae species, such as *Thaumastocyon dirus* Ginsburg, Morales & Soria, 1981 and *Agnotherium antiquum* Kaup, 1833, in which extreme modifications have been found (Morlo *et al.* 2020). Indeed, *Ammitocyon kainos* from the late Miocene of Batallones-3, Spain, a description and systematic study of which is provided by the present paper, proves that these hypercarnivorous dental adaptations were even further exacerbated in this terminal form, while also constituting the first evidence that the process also involved relevant modifications of the postcranial skeleton.

Geological setting

Batallones-3 (Fig. 1) is one of the nine palaeontological sites of the continental pseudo-karst complex developed during the late Miocene (*c*. 9 Ma) at Cerro de los Batallones, Madrid basin, Spain (Calvo *et al.* 2013). As in Batallones-1 (the first of the sites found in the area) its faunal composition is completely skewed towards an overwhelming predominance of carnivore remains, which has been explained as resulting from its role as a natural trap prior to its final sedimentary infilling (Antón & Morales 2000; Abella *et al.* 2011; Calvo *et al.* 2013; Domingo *et al.* 2011, 2012, 2013, 2016, 2018; Martín-Perea *et al.* 2020). The deposits of these sites have been dated based upon their faunistic composition as pertaining to the late Miocene (Late Vallesian, MN 10). Study of the rodents revealed the existence of minor differences in the age of the deposits, indicating

that Batallones-3 appears to constitute the most recent deposit of the series, and Batallones-10 the oldest, but within the time span of the local subzones J2 / J3 (López-Antoñanzas *et al.* 2010, 2014; Medina-Chavarrías *et al.* 2019). To date, 62 species of vertebrates have been catalogued, 47 of which are mammals (Morales 2017). Studies of the fauna of the mammal carnivorans can be consulted in Abella *et al.* (2012, 2013, 2015); Antón *et al.* (2004a, b, 2020); Fabre *et al.* (2015); Monescillo *et al.* (2014); Peigné *et al.* (2005, 2008); Salesa *et al.* (2005, 2006, 2010, 2012, 2019); Siliceo *et al.* (2014, 2015, 2017, 2019); Valenciano *et al.* (2015, 2020); for herbivorous mammals in Domingo *et al.* (2019); Pickford (2015); Ríos & Morales (2019); Ríos *et al.* (2017); Sánchez *et al.* (2009, 2011); and for other vertebrates in Vila *et al.* (2018); Morales (2017); Pérez & Murelaga (2013); Pérez-García & Vlachos (2014).

Material and methods

Nomenclature and measurements

Dental nomenclature follows Morales *et al.* (2019). Anatomical descriptions are based on Schaller (2007). Measurements (Tables 1, 2) were made using Mitutoyo Absolute digital calliper to the nearest 0.1 mm. Measurements of the cranium and mandible follow those of Siliceo (2015).

Abbreviations

BAT-1, Batallones-1 locality; **BAT-3**, Batallones-3 locality.

Institutional abbreviations

CM, Carnegie Museum of Natural History, Pittsburgh, USA; **MGUV**, Museu de Geologia de la Universitat de València, Burjassot, Spain; **MNHL**, Musée des Confluences, Lyon, France; **MNHN**, Muséum national d'Historie naturelle, Paris, France; **MNCN**, Museo Nacional de Ciencias Naturales, Madrid, Spain; **NHMMZ**, Naturhistorisches Museum Mainz/Landessammlung für Naturkunde Rheinland-Pfalz, Mainz, Germany; **NHMW**, Naturhistorisches Museum Wien, Vienna, Austria; **NMP**, National Museum, Prague, Czech Republic (inv. no. NM-Pv); **SMNS**, Staatliches Museum für Naturkunde Stuttgart, Stuttgart, Germany; **UCB**, Université Claude Bernard Lyon 1, Lyon, France; **YPM**, Yale Peabody Museum, New Haven, USA.

Studied material

The fossil remains of *Ammitocyon kainos* gen. et sp. nov. from Batallones-3 are stored in the collections of the Department of Paleobiología of the MNCN, and include: the holotype both hemimandibles of the same individual BAT-3'09.1239 and BAT-3'08.604; the paratypes BAT-3'10.1689, skull and BAT-3'11.453 complete mandible probably belonging to the same individual, BAT-3'09.1124, isolated left m2.

For comparison, we have studied the following Amphicyonidae taxa: *Magericyon anceps* Peigné *et al*., 2008 from Batallones-1 and 3; *Ysengrinia gerandiana* (Viret, 1929a) and *Cynelos lemanensis* (Pomel, 1846) from Saint Gérand le Puy (France), early Miocene (MN 2) housed in UCB and MNHN; *Peignecyon felinoides* Morales, Fejfar, Heizmann, Wagner, Valenciano & Abella, 2019 from Tuchořice (Czech Republic), early Miocene (MN 3), whose holotype (NM-Pv 11600) is stored in the collections of NMP, and the rest of the dentition are available as casts in the collections of NMP and MNCN; *Thaumastocyon dirus* Ginsburg, Morales & Soria, 1981 from Los Valles de Fuentidueña (Spain), late Miocene (MN 9) housed in MNCN;

Magericyon anceps Peigné, Salesa, Antón & Morales, 2008 from BAT-1 by cranium, mandibles and postcranial remains (Peigné *et al.* 2018; Siliceo 2015) housed at MNCN; the holotype of *Agnotherium antiquum* by a cast housed at NHMW, as well as the new mandible of the same taxon described by Morlo *et al.* (2020) and housed at NHMMZ; *Tomocyon grivensis* Viret, 1929b from La Grive Saint Alban (France), middle Miocene (MN 7/8) housed in UCB and MNHL; *Ysengrinia valentiana* Belinchón & Morales, 1989 from Buñol (Spain), early Miocene (MN 4) housed in MGUV; *Thaumastocyon bourgeoisi* Stehlin & Helbing, 1925 from Pont-Levoy (France), middle Miocene (MN 5) by casts housed in the MNHN; *Daphoenodon superbus* (Peterson, 1907) from Agate Fossil beds National Monument (USA) and *Ysengrinia americana* (Wortman, 1901) from the Harrison Formation (USA), early Miocene (late Arikarean) by casts housed in MNCN; *Pseudocyonopsis landesquei* (Helbing, 1928) from the Oligocene of Europe and *Crassidia intermedia* Heizmann & Kordikova, 2000 from the early Miocene of Europe by their original publications (von Meyer 1849; Helbing 1928; Kuss 1965; Springhorn 1997; Heizmann & Kordikova 2000; Peigné & Heizmann 2003).

Cladistic analysis

In order to analyse the phylogenetic position of the new form of Amphicyonidae from Batallones-3, we performed a cladistic analysis that included hyper- and hypocarnivorous amphicyonid taxa, such as the Oligocene *Pseudocyonopsis landesquei*, the early Miocene *Daphoenodon superbus*, *Cynelos lemanensis*, *Ysengrinia americana*, *Ysengrinia gerandiana*, *Ysengrinia valentiana*, *Crassidia intermedia* and *Peignecyon felinoides*, the middle Miocene *Thaumastocyon bourgeois* and *Tomocyon grivensis*, and the late Miocene *Thaumastocyon dirus* and *Agnotherium antiquum*. We expanded the phylogeny of Morales *et al.* (2019), including the taxa *Thaumastocyon dirus* from

Valles de Fuentidueña and *Agnotherium antiquum* from Eppelsheim, updated according to a recently described mandible (Morlo *et al*. 2020). We excluded from the analysis several taxa related to the Thaumastocyoninae, such as *Ysengrinia tolosana* (Noulet, 1876), and *Ysengrinia depereti* (Mayet, 1908), because they represent poorly sampled species. The cladistic analysis includes 13 taxa and 54 equally weighted and unordered cranial, mandibular and dental characters (see Supplemental file 1). Some of these were used by Viranta (1996), Peigné *et al.* (2008) and Morales *et al.* (2019). The complete list of characters, the character-taxon matrix and the synapomorphy list per node are available in Supplemental files 1, 2 and 3 respectively. We selected *P. landesquei* as the outgroup. The analysis was performed with PAUP*4.0b10 (Swofford 2002).

Body mass estimation

To estimate the body mass of *Ammitocyon kainos* gen. et sp. nov. we followed the methodology employed by Figueirido *et al.* (2011). We used the following formula in this study (for the femur):

$$\text{Log10 (BM)} = -1.742\ (\pm 0.310) + 2.659\ (\pm 0.249)\ \text{Log10 (Fdml)}$$

Fdml being the medio-lateral diameter of the femoral diaphysis at the mid-shaft. This measurement is one of the most suitable in this specific case, due to the extremely derived postcranial adaptations of the species.

Mandible biomechanics

In order to reconstruct the mechanical adaptations of this new genus and species we followed the methodology performed by Hunt (2011) in the also hypercarnivorous

Temnocyoninae (Amphicyonidae). We employed the methodology of Therrien (2005) whereby the carnivoran mandible was modelled as a solid beam, used to represent relative differences in biomechanical properties along the mandible, thus indicating its resistance to forces applied during feeding and prey capture. Zx/Zy values are a measure of relative bending strength on the sagittal and transverse planes of the mandibular corpus considered by Therrien (2005) as mandibular force profiles. Therefore, these Zx and Zy ratios estimate the relative differences between parasagittal and transverse loadings along one single mandible with the advantage that these patterns can then be compared among carnivoran species. Comparison of Z/L ratios for different taxa reveals variations in the magnitude of applied force at different locations along the mandible, while the ratio Zx/Zy reflects the relative mandibular force (or overall mandibular shape). Furthermore, since Zx/Zy is proportional to the ratio of the dorsoventral and mediolateral diameters of the mandibular corpus, a ratio < 1.00 indicates an adaptation toward bucco-lingual loads (wider than the deep mandibular corpus). These forces are interpreted as an adaptation to stresses induced while biting prey, either due to struggling motions or to other transverse or torsional stresses produced by hard objects (Therrien 2005). We included the living species *Canis lupus* (grey wolf), *Crocuta crocuta* (spotted hyena) and *Panthera leo* (African lion) together with the indices from Hunt (2011) and the measurements of the lower jaw of *M. anceps* from BAT-1 (Table 3). This enabled all these amphicyonids to be compared and further evaluated to establish whether the adaptations to supposedly similar food sources were similar among these groups.

Systematic palaeontology

Order **Carnivora** Bowdich, 1881

Suborder **Caniformia** Kretzoi, 1943

Family **Amphicyonidae** Trouessart, 1885

Subfamily **Thaumastocyoninae** Hürzeler, 1940

Genus ***Ammitocyon*** gen. nov.

Diagnosis. Thaumastocyoninae with sectorial dentition, dental formula 3/3, 1/1, 2/1, 2/2, mandible presenting a long diastema between canine and p4, p4–m2 with strong bucco-lingual compression, p4 of moderate size with small mesial cuspid and large distal cuspid, m1 with short and low paraconid, absent metaconid, talonid short and narrow, occupied by a strong hypoconid, the entoconid reduced to a weak buccal cingulum; m2 relatively elongated, with a similar arrangement of the cuspids (paraconid, protoconid and hypoconid) to that of the m1. Upper canine robust with bucco-lingual compression, P4 elongated with a large parastyle (inferred) and lingual root for the protocone well developed and placed transversely to the mesial-distal molar axis. Furthermore, the M1 and M2 are reduced, displaying a triangular occlusal shape. Postcranial robust, especially the bones of the zygopodial and autopodial segments. Towards the distal parts of the limb the articulations become gradually less mobile, some of these ankylosed or even completely immobile. All phalanxes short, ungual phalanxes short with a rounded outline, and with a short and thickened claw.

Differential diagnosis. *Ammitocyon* differs from the rest of the genera included in Thaumastocyoninae (*Crassidia*, *Peignecyon*, *Thaumastocyon*, *Tomocyon* and *Agnotherium*) in the following autopomorphies: a very high position of the masseteric fossa in the mandibular ascending ramus; development of a wide flattened surface in the

premasseteric area; a horizontal mandibular ramus with the concave *margo alveolaris* in its central part; a lower postcanine dental row which is not rectilinear but rather arranged in a sigmoidal manner, the consequence of the imbrication of the distal part of the p4 with the buccal base of the paraconid of the m1, and the change in orientation of the m2, which turns in relation to the mesial-distal axis of the mandible, in such a way that its trigonid is displaced lingually and the talonid is shifted buccally. The m2 is elongated with a very well-developed paraconid, displaced towards a mesio-lingual position, the metaconid is missing and the entoconid is very reduced.

Derivation of name. The epithet 'Ammit' refers to the name of a demoness and goddess in ancient Egyptian religion who was part crocodile, lion and hippopotamus, traits that are reminiscent of the proposed new genus, and 'cyon' from the Greek term for dog.

Age. Late Miocene (MN10).

Ammitocyon kainos sp. nov.

(Figs 2–4)

2017 *Thaumastocyon* sp. Morales, Abella & Valenciano: 340, Figures 7–8.

2019 *Thaumastocyon* sp. Morales *et al.*: 399.

2020 *Thaumastocyon* sp. Morlo *et al.*: 4.

Holotype. BAT-3'09.1239 and BAT-3'08.604, mandible with both rami.

Paratypes. BAT-3'10.1689, skull and BAT-3'11.453 complete mandible, probably belonging to the same individual. BAT-3'09.1124, isolated left m2.

Type locality. Batallones-3, Madrid, Spain.

Derivation of name. Kainos from the Greek term for 'of a new kind'.

Diagnosis. As for the genus.

Age. Late Vallesian, MN10, local zone J.

Description

Skull. The sample consists of a single skull from the senile specimen BAT-3'10.1689 (Fig. 2). It is relatively robust, and although it is severely corroded, especially in its dorsal region, many of its structures can be still described in detail. Compared to *Magericyon anceps* (Peigné *et al*. 2008) the premaxilla is robust and possesses a battery of bucco-lingually enlarged incisors (Supplemental file 4). The nasal bone is thick and is rostrally protruded, forming a huge snout, with a wide nasal aperture. In dorsal view, the snout is somewhat isolated from the rest of the skull by a deep notch on the outline just rostral to the P4, which is laterally expanded. Most of the frontal and maxillary bones are completely corroded, and many of the structures cannot therefore be described. This is the case of the infraorbital foramen, in which only a deep depression at the level of the mesial-most part of the P4 can be observed. The rostrum has an '8'-shaped general outline in ventral view, with an enlarged rostral-most region, a narrower area at the level of the P1 and the diastema and a wide and rounded caudal region

between the P4 and the M2. The palate is caudally expanded, exceeding the level of the last molars, a feature shared with *Ysengrinia americana* and some Temnocyoninae (Hunt 2002, 2011). In addition, the postorbital processes both of the frontal and of the jugal are well developed. This configuration results in a relatively large eye socket, much more enclosed than in other closely related large-sized arctoid carnivorans. The postorbital constriction is well marked, completely delimiting the frontal and the parietal bones. In lateral view, the zygomatic arch is relatively thin and straight, only curving ventrally towards the last portion of the squamosal bone. In dorsal view, the rostral-most part of the jugal is enlarged, forming a flat surface throughout the ventral part of the eye socket. The postglenoid process is located higher than the mastoid process. The basicranium is wide and expanded at the level of the mastoid processes. The posterior opening of the alisphenoid canal and the foramen ovale are close to each other; as in other similar forms such as *Magericyon* (see Peigné *et al*. 2008) they are located medial to the preglenoid process. The postglenoid foramen is large and is located just caudal to the relatively thin and ventrally projected caudal wall of the postglenoid process. The auditory region is anteroposteriorly short and is delimited by the postglenoid and the mastoid process, forming a dorsally projected, oblique and narrow auditory notch (Supplemental file 5). The bulla is thick and somehow inflated. Meatal tube long and dorsally projected, with a longitudinal groove. The mastoid process is robust and prominent; it is laterally inflated and rugose. On its dorsal side a very smooth concave structure can be observed. The paraoccipital process is robust and projected caudo-ventrally, surpassing the ventral edge of the mastoid process (Supplemental file 5). The sagittal crest is well developed and convex, arising from the postorbital constriction towards the nuchal crests. These are developed in height, but due to severe corrosion of this portion of the skull, their lateral expansions cannot be

evaluated. The parietal region is quite convex and is located in a relatively distal and ventral position, in relation to the frontal region.

Upper dentition. The only preserved upper dentition belongs to the previously described skull BAT- 3'10.1689 (Fig. 2, B- B'). As occurs with the lower dentition of this specimen, it is well worn and some of the morphological features have been blurred (Fig. 2, F and G). The incisor battery is extremely wide (Fig. 2, B-B'), each one well separated from the other, similar to what can be observed in derived barbourofelids (e.g. Tseng *et al.* 2010; Robles *et al.* 2013). The I3 is clearly larger than the I2 (no I1 is recovered, but the size of the alveolus would appear to indicate that is clearly smaller than the I2). Their most remarkable feature is their strong bucco-lingual width, much more developed than that of any of the compared carnivorans (Table 1). As with the rest of the dentition, they exhibit a high degree of wear. The canines are robust, with a wide base and a moderate height. They display two vertical wear facets, one distal and another in mesio-lingual position. The buccal wall is clearly convex and the lingual wall is somewhat flattened. In the mesial-most part of the diastema a small residual P1 is present; it has no homologue tooth in the lower dentition and its function is therefore unclear. Both carnassials are extremely worn, the right one almost down to its roots, while the left one still shows the buccal wall (Fig. 2). Most likely the protocone was still quite well developed, judging by the size of its root; it is located in a relatively distal position, possibly due to the strong development of the parastyle. In the left row, both the P4 and the M1 show a strong oblique wear facet, reaching the base of the protocone. The M1 would seem to have been relatively small, presenting a marked triangular outline; in the buccal wall a moderate cingulum is present. The right row has conserved an eroded M2. The only visible feature appears to involve its relatively small size and

its triangular outline. No alveoli are observed for the M3, but the caudal part of the maxillary bone is rather poorly preserved.

Mandible (Fig. 3). The sample consists of two complete adult mandibles: BAT-3’09.1239 and BAT-3'08.604 (holotype) and BAT-3’11.453, with a highly worn dentition, which probably belongs to the same individual as the BAT-3’10.1689 skull. The mandible is robust and long, with a strong symphysis; it is relatively dorso-ventrally slender between the canine and the p4, and bucco-lingually very thick under both m1 and m2. The *margo interalveolaris* is sharp and in lingual view it displays a concave profile, common in species with reduced premolars, and presents a long diastema between the lower canine and the enlarged p4. There is only one well-developed mental foramen, located below the postcanine diastema. In lateral view, the ventral border of the mandibular body shows several points of inflexion, as it is convex at the symphysis and under the m2; it is concave at the level of the diastema and the p4. The distal-most region of the mandibular corpus, including the angular process, is shifted towards the lingual side of the mandible, forming a marked convex structure in ventral view. Consequently, the angular process is short and rounded, with a blunt distal edge. The articular process is robust, and short along the latero-medial axis. The articular facet for the skull is large and occupies practically the entire medial region. The coronoid process is moderately developed in height but antero-posteriorly quite large. It is orientated dorsally and has a verticalized posterior border, with a rather flat dorsal tip. The masseteric fossa is located in an unusual position, starting at the level of the dentition, contrary to what can be observed in almost all of the carnivorans, where it is expanded ventrally. It is completely enclosed in its ventral region by a relatively deep rim that separates the fossa itself from a flat region situated in a position analogous to

the premasseteric fossa of some Ursoidea. The *masseter* muscle insertion area is relegated to the most caudal corner of the ventral edge of the angular process. There is a flat part between the masseteric fossa and the insertion of the digastric; it is very large in one of the specimens, although it is not lingually expanded as can be seen in bears.

Lower dentition (Fig. 4). No incisors are preserved, but the right ramus preserves the alveoli, the i3 is mesio-distally enlarged and is placed mesially to the smaller i2 and i1 alveoli. The canine has a robust root, with a high and relatively slender crown; a well-developed mesio-lingual cristid, and another distal one that it is badly worn. The mesial premolars (p1–p3) are missing, and as a result the diastema between the canine and the p4 is long. The p4 is relatively large compared to the m1. It has a blunt mesial accessory cuspid, slightly rotated lingually. The main cuspid is projected distally, showing a marked and deep wear surface in its buccal wall that is large and was likely moderately bucco-lingually compressed. The distal cuspid is relatively enlarged, and also exhibits a strong wear facet on its buccal wall. Both the distal cuspid of the p4 and the mesial wall of the paraconid of the m1 are imbricated, slightly tilting the m1lingually.

The m1 is a rather simple tooth, with a mesio-distally aligned paraconid, protoconid and hypoconid. The paraconid of the m1 possesses a large and well-developed cingulum at the base of its lingual wall, while the buccal one is completely smooth. There is quite a notable difference in height between the paraconid and protoconid, which is taller. However, they share a large vertical wear facet on the buccal wall. The mesial crisitid of the paraconid is displaced slightly towards a more lingual position; it is subdivided and well isolated. The distal cristid of the protoconid is visibly sharp as a consequence of a bucco-distal vertical wear facet. A slight inflexion in this cristid marks the place for the metaconid, which, however, is completely reduced. The

talonid is short and narrow, and buccally well separated from the trigonid by the previously described wear facet. It is formed by a huge hypoconid with an oblique wear facet, slightly tilted lingually, which practically occupies the whole cuspid. It also has a lingual basal cristid, almost a cingulid, which runs from the posterior short cristid of the hypoconid towards its lingual base. Its basal cingulid is quite small, both on its lingual and buccal walls.

The m2 is elongated, with the same cuspid alignment as the m1, and is missing the metaconid. The paraconid is large and lingually placed, somewhat imbricated with the hypoconid of the m1. The protoconid is rounded and pyramidal and the talonid is severely worn. It functions as the distal-most occlusal region since this species lacks an m3.

Postcranial skeleton (Fig. 5; Supplemental file 6). A description of the postcranial bones and the functional anatomy of this new genus and species will be provided in a subsequent manuscript. However, due to the extreme adaptations found in the skeleton of *A. kainos*, a preliminary characterization of the recovered bones has been performed in order to establish the palaeobiology of this species as a whole.

The scapula is robust and almost square in overall shape. It has a large subscapularis fossa and a scapular spine, the latter occupying the whole length of the scapula. The acromiom is dorsally developed but does not surpass the glenoid cavity. The humerus is robust, with a long wide deltoid tuberosity and a large lateral supracondylar crest. It has no entepicondylar foramen. Its distal epiphysis is wide. The radius and ulna are robust and short, with large muscular attachments along its diaphysis. The manus is robust and short, especially towards the distal segments. Relatively short and robust carpals, short and robust metapodials with flattened distal

epiphysis and extremely robust phalanxes, especially the distal ones, which present an almost rounded section. Articulation between the trapezium and Mc I rounded in section but completely flat. Pelvis robust, although too fragmented to describe. Femur fragmented, although it possesses sufficient complete parts to describe it as robust and relatively short. Distal epiphysis wide and robust. Tibia robust and with wide proximal epiphysis; with a short diaphysis. Distal epiphysis with a triangular section and with relatively oblique, deep and reinforced articulation sulci for the astragalus. Pes wide and short, especially towards the distal segments as in the manus. Tarsals robust and with few contact facets. Calcaneus short with solid articulation facets for the astragalus and a concave distal one for the cuboid. Astragalus with almost no distal neck and almost rounded and convex articular facet for the navicular. No articulation facet between the cuboid and navicular. Short and robust metatarsals with a flattened distal epiphysis. Extremely robust phalanxes, especially the distal ones, which are almost rounded.

Discussion

Ammitocyon kainos gen. et sp. nov. has all the necessary morphological traits for consideration as the most derived thaumastocyonine (*sensu* Morales *et al.* 2019). It differs from all the other members of the subfamily (*Crassidia*, *Ysengrinia*, *Peignecyon*, *Tomocyon*, *Thaumastocyon* and *Agnotherium*); consequently, a new genus and species have been erected. Comparisons with these Thaumatocyoninae are necessarily limited to dentition and mandible, since there is currently no cranial material that can be clearly attributed to any of the species of the group.

The known mandibles of the Thaumastocyoninae species (Stehlin & Helbing 1925; Viret 1927; Heizmann & Kordikova 2000; Morales *et al.* 2019; Morlo *et al.*

2020) show the typical morphology of the Amphicyonidae, in which the depth of the masseteric fossa surpasses the basal level of the postcanine row, to a greater or lesser extent approaching the mandibular border (*margo dorsalis*) and clearly differ from the distinctive morphology of *A. kainos* in which the lower edge of the masseteric fossa does not exceed the depth of the *margo alveolaris*. The unique development of a wide flattened surface in a premasseteric position in the mandible of *A. kainos* is difficult to interpret. In any case, it does not seem to be a homologous structure in the other mandibles attributed to the Thaumastocyoninae species. Another autapomorphy also present in the mandible of *A. kainos* involves the development of a broad inflection or concavity in the *margo dorsalis*, which extends from the genial tuberosity to the mesial base of the ascending ramus. The sigmoidal arrangement of the postcanine row in the *margo alveolaris* of the mandible of *A. kainos* is also unique among the Thaumastocyoninae, in part as a consequence of the broad overlap between the distal part of the p4 and the lingual base of the paraconid of the m1, but also because of the rotated arrangement of the m2, whose paraconid contacts the disto-lingual base of the talonid of the m1. In *Agnotherium antiquum* from Charmoille (Morlo *et al.* 2020) the p4 smoothly overlaps the buccal base of the m1 paraconid, but both teeth still maintain a linear arrangement in the *margo alveolaris*. The m2 of *A. kainos* differs from the other species of the group in the greater size and height of the paraconid, which is buccally located towards a position analogous to that of the m1 paraconid. The loss of the metaconid and the narrowing of the lingual area of the talonid endow the m2 of *A. kainos* with the appearance of a small-sized lower carnassial.

Some other characters of *A. kainos* reach a more specialized level than those of other species of the group; as is the reduction of p1–p2, which is present not only in Thaumastocyoninae, but also in another Amphicyonida; however, in *A. kainos* it

presents an extreme degree, with the disappearance of all the lower premolars between the canine and the p4. The main cuspid of the p4 of *A. kainos* is distally projected; a morphology that is already manifested in *Peignecyon felinoides* and all more recent species. The reduction of the postcanine dentition is one of the typical characteristics of the Thaumastocyoninae. It is possible that *A. kainos* lacks the lower third molar, since in the existing mandibles no alveolus is distinguished for this tooth. However, the state of preservation of the skull does not unequivocally indicate the absence of the M3, although it is likely due to the extreme reduction of the M2. In the lower dentition, the m2 is greatly reduced in Thaumastocyoninae, and in *Agnotherium antiquum* from Eppelsheim the reduction is very advanced (Morlo *et al.* 2020), as in *Thaumastocyon burgeoisi* and *Th. dirus* (Stehlin & Helbing 1925; Ginsburg *et al.* 1981). However, in *A. kainos* the morphological pattern of m2 differs from the rest of the species in the group, as has already been mentioned. The morphology of the upper dentition of *A. kainos* is only preserved in the one single skull discovered; which presents a high degree of wear, characteristic of an elderly individual, as well as evidence of corrosion. However, the P4 has a large parastyle, and an elongated cutting blade formed by the paracone and metastyle; furthermore, both cusps are supported by two merged hypsodont roots. Furthermore, both the M1 and the M2 are greatly reduced compared to the P4, exhibiting a triangular outline similar to that of the M1 of *Thaumastoyon* species. This combination of such derived features has no known equivalent in the remaining Thaumastocyoninae; in *Crassidia intermedia*, *Ysengrinia gerandiana* and *Peignecyon felinoides* the morphological pattern is still close to that of other Amphicyoninae, although an incipient hypercarnivorous tendency can be inferred. Unfortunately, in the most recent species of the subfamily, the only known upper dentition consists of isolated teeth, a fact that hinders comparison, and in some cases casts doubt upon their

association with a given species; as is the case of *Tomocyon grivensis* from the La Grive-St-Alban karst site (Viret 1927), which possesses a very sectorial P4 and m1, but little reduction in the grinding molars (m2 and M1); this constitutes a mixture of hyper- and hypocarnivorous traits (Kuss 1962; Morales *et al.* 2019). The description of the new Eppelsheim mandible attributed by Morlo *et al.* (2020) to *Agnotherium antiquum*, with an m2 still encrypted in the alveolus presenting a strong reduction in size with respect to m1, rejects the proposal by Kuss (1962) to include *Tomocyon grivensis* in *Agnotherium*. However, this fact does not dispel the doubts regarding the peculiar character of *Tomocyon*, a species comprising isolated dentition, from different diachronic karst fillings, in which at least three large-sized Amphicyonidae species were present (Mein & Ginsburg 2002).

The differences between *Ammitocyon kainos* and all the other genera included in the Thaumastocyoninae justify the erection of a new genus and species from the Batallones-3 fossils.

Phylogenetic relationships

The phylogenetic relationships of the Thaumastocyoninae have recently been discussed by Morales *et al.* (2019) in relation to the description of *Peignecyon felinoides* (from the early Miocene site of Tuchořice, Czech Republic). This species is crucial with regard to understanding the beginning of the Thaumastocyoninae clade because of the abundant material, including upper and lower dentition. The new phylogenetic analysis is based on that published by Morales *et al*. (2019), with the addition of new characters and three taxa, *Agnotherium antiquum* —including the new mandible described by Morlo *et al*., (2020) —, *Thausmastocyon dirus* (Ginsburg *et al*., 1981) and *Ammitocyon kainos*. gen.

et sp. nov. — the former two species were considered as one single taxonomic unit in the previous analysis under the name of *Thaumastocyon* spp. —. The Thaumastocyoninae clade (node B) can be recognized since the early Miocene with *Crassidia intermedia*, *Ysengrinia gerandiana* and *Peignecyon felinoides* (Figs 6, 7). In this clade, the reduction of second molars (m2 / M2) begins to be detected, a trend that will be accentuated in successive dichotomies in the direction of a more hypercarnivorous adaptation (including the modification of the carnassials: m1/P4). This morphological trend was almost fully achieved at the beginning of the middle Miocene with *Thaumastocyon bourgeoisi* from the locality of Pont Levoy, France (Stehlin & Helbing 1925), in which the reduction of the m2 in relation to m1 reaches its maximum, and the m1 reveals the morphology of the more derived forms of the group such as *Agnotherium antiquus* or *Ammitocyon kainos*. The M1 of *Th. bourgeoisi* shows the morphology that will characterize the most recent hypercarnivorous species, with a strong reduction of the lingual area, which is limited to a vestigial lingual cingulum. The species *Thaumastocyon dirus* Ginsburg *et al.* (1981) from the early late Miocene (MN9) of Spain preserves the M1 morphology of *Th. bourgeoisi*, although it is even more specialized, a fact that can be seen especially in the greater relative development of the buccal cusps (paracone and metacone) and the definitive loss of the lingual cingulum. *Thaumastocyon* species appear as a sister group to *Ammitocyon*, and this relationship is strongly supported, despite the scarcity of data on *Th. dirus*. Further difficulties arise with *Agnotherium antiquum*, originally only represented by an m1 presenting a high degree of wear, to which Morlo *et al.* (2020) added new data from a sub-adult mandible from the same locality. However, its phylogenetic position is not well resolved due to the absence of the upper dentition. Another taxon posing a similar difficulty is *Ysengrinia valentiana*, a species represented by two molars (M1 and m2)

(Belinchón & Morales 1989). These molars are morphologically transitional between those of *Peignecyon felinoides* and *Th. bourgeoisi*, but the absence of information on the morphology of the carnassials prevents a more accurate systematic position. *Tomocyon grivensis* possesses a mixture of primitive and derived characters, and is placed in the cladogram in a position that represents this duality; the sectorial carnassials bring it closer to *Thaumastocyon* and *Ammitocyon*, but the retention of large molars (M2 and m2) anchors it to the more primitive species of the group. It likely plays an important role, or at least contributes to the unresolved topology of the more derived species of the clade.

Finally, the polyphyly detected in *Ysengrinia* is once again evidenced in this cladistic proposal, as previously discussed by Morales *et al.* (2019). The species *Ysengrinia valentiana* cannot be considered within this genus, being closer to *Peignecyon* or *Thaumastocyon* than to the type species *Ysengrinia gerandiana*. Similarly, *Ysengrinia americana* (see Hunt 2002; Morales *et al*. 2019) should be excluded from *Ysengrinia*. This species presents a dental morphotype displaying a lower degree of hypercarnivorism, clearly independent from both Thaumastocyoninae and Haplocyoninae. Morphotypes close to *Ysengrinia americana* have been recorded in Asia by Qiu *et al*. (1986), who determined a maxilla and an m1–m2 from Shanwang, China as Thaumastocyoninae gen. et sp. nov.; it was subsequently redetermined as *Ysengrinia* sp. by Qiu & Qiu (2013); *Ysengrinia* sp. has also been recorded in the Bihoku group, Hiroshima (Japan) on the basis of an M1 morphologically close to *Ysengrinia americana* (Kohno, 1997). Nonetheless, it is difficult to relate them to each other, although their exclusion from Thaumastocyoninae would seem to be clear. The basal position of *Ysengrinia americana* which constitutes a tricotomy with the Thaumastocyoniae and the clade *Cynelos-Daphoenodon* could be interpreted as a

persistence of an ancestral hypercarnivore dentition during the Miocene in North America and Asia. The other two branches of the trichotomy show divergent dental morphologies, one towards extreme hypercarnivorism (Thaumastocyoninae) and the other less hypercarnivorous in which the postcarnassial teeth show an increase in size (Amphicyoninae). The latter species will give rise to to the major Amphicyoninae cladogenesis during the Miocene (Kuss 1965; Viranta 1996; Hunt 1998; Ginsburg 1999; Peigné *et al*. 2008; Werdelin & Peigné 2010).

Palaeobiology approach

Ammitocyon kainos gen. et sp. nov. represents the most complete Thaumastocyoninae known in the fossil record. Following the methodologies used by Figueirido *et al*. (2011), who employ measurements of the postcranial skeleton, we estimated at 231 kg the body size of the available specimen of *Ammitocyon kainos*. This value is within the range of the estimation of body size obtained for this same specimen in Domingo *et al.* (2016), rendering this species one of the top three largest carnivoran species of the whole BAT-3 carnivoran guild, comparable to the sabre-tooth felid of a lion-sized *Machairodus aphanistus* (Kaup, 1832), and the brown bear-sized ursid *Indarctos arctoides* (Depéret, 1895). *Ammitocyon* was larger than *Magericyon anceps* and presented a different morphological adaptation despite the hypercarnivorous adaptation of both species. A significant contribution with regard to understanding the habitat and palaeobiology of these large predators was provided by means of analysis of the carbon stable isotopes in tooth enamel from carnivorous and herbivorous species from BAT-1 and BAT-3 (Domingo *et al*. 2016, 2017). In relation to *Ammitocyon*, we can extract some relevant conclusions from these studies: (1) there are no major differences in the

surrounding areas of the Batallones sites, dominated by C3 plants, woodland habitat with patches of wooded grassland; these conditions were similar in the Los Valles de Fuentidueña site (locality type of *Thaumastocyon dirus*), which is slightly older than the Batallones localities; (2) the data suggest that the principal available food resource for the large predators was the equid *Hipparion*, and that the interspecific competition was therefore very high, particularly in BAT-3, with its higher number of large sympatric carnivores; (3) *Magericyon anceps* is the only species from BAT-3 to show significant differences with regard to prey, possibly hunting in a more open habitat. This highlights the divergence between the two BAT-3 amphicyonids.

The masticatory apparatus of *A. kainos* is unique among those known in amphicyonids, lacking a clear correspondence with other mammalian hypercarnivores. Many traits of this genus can be found in other hypercarnivorous species, but they are not mutually associated. The new genus presents an unequivocal tendency towards the dental simplification and the postcanine functional dentition comprising only p4–m2 (lower) and P4–M2 (upper). The carnassial function comprises a p4–m1 that occludes with an elongated P4 by extending the parastyle and metastyle. But a functional 'secondary carnassial pair' is formed by the m1 talonid and the m2, both of which occlude with the M1–M2 buccal wall. Postcarnassial (P4/m1) dentition in hypercarnivores mammals is reduced, becoming almost totally lost in Feliformia (felids, hyaenids and some viverrids), or strongly reduced in some Caniformia (e.g. Mustelidae) (Ewer 1973). A distant analogy was detected in *Ammitocyon* with the molar dentition of some creodont hyaenodonts but the phylogenetic distance and the great diversity and complexity of this group prevented us from interpreting this singular parallelism. The mental region is robust, presenting large curved canines, elongated bucco-lingually and with broad roots relative to the height of the crown. Additionally, the loss of the

premolars in the mandible is not accompanied by a shortening of the *margo interalveolaris*. This combination of robust incisors and canines with sectorial and slender postcanine dentition could be considered as a feature common to the Thaumastocyoninae, although in *Crassidia* and *Thaumastocyon* it is not as derived as in *Ammitocyon*. Indeed, the postcanine dentition in *Ammitocyon* reaches a very advanced degree of sectorialization. The masticatory muscles and functional anatomy of the cranio-mandibular articulation also displays certain singularities. Noteworthy among these are the narrowing of the insertion of the *M. masseter* in the mandible, and especially the almost complete reduction of the attachment area for the *M. masseter pars zygomaticomandibularis posterior* in the mandible (following the nomenclature of Brassard *et al.* 2020). The latter muscle constitutes the main grinding component of the jaw movements in several carnivorans (Davis 1964). Therefore, the loss of this muscle insertion area, together with the large development of the *temporalis* and *digastricus* muscles could be an anatomical response, favouring slicing vs. the chewing, a fact that allies well with the general morphology of the teeth. Conversely, the bio-mechanical analysis performed in the present paper supports the hypothesis that the mandible of *A. kainos* was much more resistant to medio-lateral movements than to dorso-ventral ones, the region just mesial to the p4 constituting the least resistant part of the mandible, and the symphysis being the only part capable of resisting both dorsoventral and lateral movements (Fig. 8; Table 3). The values obtained in both Zx and Zy show large differences in relation to those of the canids and amphicyonids measured in both Therrien (2005) and Hunt (2011). Indeed, these values occupy an empty morphospace in relation to this carnivoran sample; conferring to the mandible both much more resistance to medio-lateral bending but less dorso-ventral resistance than any of the compared extant and extinct carnivorans (Therrien 2005; Hunt 2011). This has several

important consequences in the biomechanics of the mandible with regard to the forces at play during hunting and feeding in *Ammitocyon kainos*.

In the first place, the muzzle possesses greater bucco-lingual and dorso-ventral resistance than the other species (Fig. 8). This could be related to the large incisors and wide canines, which act as a throat or muzzle clamp and which would help to hold and tear any outer layer of skin in the prey. This represents a completely different hunting model than that of the canine shear bite of the large machairodontines (Antón *et al*. 2011). Furthermore, the low level of resistance to dorso-ventral bending of the mandibular corpus in the postcanine means that it was likely unable to feed on hard matter. This is consistent with the dental adaptations of this area of the jaw, in which the P4 and m1 act as a shearing surface and the M1 and m2 as an independent second cutting area. Finally, the large bucco-lingual resistance to bending along the whole mandibular ramus was probably related to the ability to tear off pieces of flesh while biting and moving the head from side to side with violent movements, similar to those performed by pinnipeds (Ewer 1973; Hocking *et al.* 2013, 2017).

The robustness of the postcranial skeleton of *A. kainos* can exceed that of bears in many cases (Ewer 1973). Indeed, it has several features in common with the skeleton of the extinct saber-toothed metatherian *Thylacosmilus atrox* Riggs, 1934, with its relatively short limbs and short (and spreading) metapodials (Ercoli *et al.* 2012; Janis *et al.* 2020). Some of the bones possess strengthened articulations that prevent lateral movements between bones, especially in the hind limb. These limitations are not only found at the ligament level; limiting bone structures can also be observed, such as developed crests and contact facets, especially among the zygopodium and autopodium; some of which are similar to those observed in cursorial mammals (Barone 1999, 2000; Bertram 2016; Bohmer *at al.* 2020). The manus and pes are robust and short, with

cramped metapodials that would have also limited lateral movements; some of these even lack any flexing capacity (e.g. digit I in the manus). Finally, the sturdy phalanxes are one of the most surprising features, since they are so short that they could not be assembled into a digitigrade position, since the resulting surface was too small to support this animal's large body mass (Bertram 2016). However, when reconstructed as a plantigrade there are also several discrepancies in the anatomy that cannot be addressed until more detailed comparisons of its postcranial skeleton are made.

Conclusions

Ammitocyon kainos gen. et sp. nov. represents both the most recent and the most complete member of the subfamily Thaumastocyoninae. It extends its temporal record until the late Vallesian (*c*. 9.1 Ma), and contributes to updating our understanding of the thaumastocyonine lineage. The results of our phylogenetic analysis prove that this new form reached the maximum specialization within the Thaumastocyoninae, a group that includes the most hypercarnivorous Amphicyonidae species of the Miocene. *Ammitocyon kainos* (Fig. 9) can be interpreted as a chimerical carnivoran combining one of the more hypercarnivorous dentitions from the suborder Caniformia, a large body size and of one of the most robust postcranial skeletons of the group.

At present, the general skeletal adaptations and body size of *A. kainos* might suggest that this species acted as an occasional stalking hunter of large prey, or even a kleptoparasite of other more active large carnivore hunters. The powerful bite of the muzzle and some of its postcranial adaptations (for example, strong forearms and sturdy hind limbs) would have helped both behaviours. However, there is a need for further

anatomical studies of the complete skeleton in order to fully reconstruct a more detailed model of its ecomorphology.

Acknowledgements

We are grateful to the following curators and collection managers for providing access to the comparative material in their care: S. Fraile (MNCN), D. Berthet and F. Vigouroux (MNHL), C. Argot (MNHN), U. Göhlich (NHMW), O. Fejfar and J. Wagner (NMP), and P. Mein (UCB). We also wish to thank Dr. Robert M. Hunt Jr. (University of Nebraska State Museum) for providing casts of *Ysengrinia americana* and *Daphonoedon superbus*, and M. Morlo (Senckenberg Research Institute) for his interesting contributions and providing access to the mandible of *Agnotherium antiquum*. We are also indebted to D. Hontecillas (MNCN) for kindly sharing updated pictures of *Tomocyon grivensis* from La Grive Saint Alban (France) housed in MNHL. We would like to thank E. Cantero for his excellent preparation of some of the fossil remains. The present study was supported by the Spanish Ministerio de Economía y Competitividad (Research Projects PGC2018-094122-B100 and CGL2016-76431-P) (AEI/ FEDER, UE), the Research Groups CSIC 64 1538 and CAM-UCM 910607, the Generalitat de Catalunya (CERCA Programme, and Beatriu de Pinós contract 2017 BP 00223 from AGAUR to JA), and Gobierno de Aragón (E33_17R). Additionally, our research received funding from the SYNTHESYS Project http://www.synthesys.info/, which is financed by European Community Research Infrastructure Action under the FP7 ‘Capacities’ Program under the grant agreement (SYNTHESYS; CZ-TAF-3329) with JA. The ‘Juan de la Cierva Formación’ program (FJC2018-036669-I), from the Spanish Ministry of Science, Innovation, and Universities also funded AV. We thank

Cormac De Brun for the thorough language review. The editor Z. Johanson, and the reviewers Dr. Morlo and 'anonymous reviewer 2' are also acknowledged for their valuable comments, which helped to improve the final version of the manuscript.

Supplemental material

Supplemental material for this article can be accessed at:

References

Abella, J., Domingo, M. S., Valenciano, A., Montoya, P. & **Morales, J.** 2011. La asociación de carnívoros de Batallones 3, Mioceno Superior del Cerro de los Batallones, Cuenca de Madrid. *Paleontologia i Evolució, Memòria Especial*, **5**, 21–24.

Abella, J., Alba, D. M., Robles, J. M., Valenciano, A., Rotgers, C., Carmona, R., Montoya, P. & **Morales, J.** 2012. *Kretzoiarctos* gen. nov., the oldest member of the giant panda clade. *PLoS ONE*, **7**(11), e48985, doi:10.1371/journal.pone.0048985

Abella, J., Valenciano, A., Pérez-Ramos, A., Montoya, P. & **Morales, J.** 2013. On the socio-sexual behaviour of the extinct ursid *Indarctos arctoides*: an approach based on its baculum size and morphology. *PLoS ONE*, **8**(9), e73711, doi:10.1371/journal.pone.0073711

Abella, J., Pérez-Ramos, A., Valenciano, A., Alba, D. M., Ercoli, M. D., Hontecillas, D., Montoya, P. & **Morales, J.** 2015. Tracing the origin of the panda's thumb. *Science of Nature*, **102**(35), 1–13.

Antón, M. & **Morales, J.** 2000. Inferencias paleoecológicas de la asociación de carnívoros del yacimiento de Cerro Batallones. *Arqueología, Paleontología y Etnografía*, **6**, 190–201.

Antón, M., Salesa, M. J., Morales, J. & **Turner, A.** 2004. First known complete skulls of the scimitar-toothed cat *Machairodus aphanistus* (Felidae, Carnivora) from the Spanish late Miocene site of Batallones-1. *Journal of Vertebrate Paleontology*, **24**, 957–969.

Antón, M., Salesa, M. J., Pastor, F., Sánchez, I. M., Fraile, S. & **Morales, J.** 2004. Implications of the mastoid anatomy of larger extant felids for the evolution and predatory behaviour of sabretoothed cats (Mammalia, Carnivora, Felidae). *Zoological Journal of the Linnean Society*, **140**, 207–221.

Antón, M., Salesa, M. J., Pastor, J. F., Peigné, S. & **Morales, J.** 2006. Implications of the functional anatomy of the hand and forearm of *Ailurus fulgens* (Carnivora, Ailuridae) for the evolution of the "false-thumb" in pandas. *Journal of Anatomy*, **209**, 757–764.

Antón, M., Siliceo, G., Pastor, J. F., Morales, J. & **Salesa, M. J.** 2020 The early evolution of the sabre-toothed felid killing bite: the significance of the cervical morphology of *Machairodus aphanistus* (Carnivora: Felidae: Machairodontinae). *Zoological Journal of the Linnean Society*, **188**, 319–342.

Barone, R. 1999. *Anatomie comparée des mammifères domestiques, tome 1, ostéologie*. Fourth edition. Éditions Vigot, Paris, 761 pp.

Barone, R. 2000. *Anatomie comparée des mammifères domestiques, tome 2, Antrologie et Myologie*. Fourth edition. Éditions Vigot, Paris, 1021 pp.

Belinchón, M. & **Morales, J.** 1989. Los carnívoros del Mioceno inferior de Buñol (Valencia, España). *Revista de Paleontología*, **4**, 3–8.

Bertram, J. E. A. 2016. *Understanding mammalian locomotion: concepts and applications*. Wiley-Blackwell, Hoboken, New Jersey, 407 pp.

Boardman, G. S. & **Hunt, R. M. JR.** 2015. New material and evaluation of the chronostratigraphic position of *Daphoenictis tedfordi* (Mammalia, Carnivora, Amphicyonidae), a cat-like carnivoran from the latest Eocene of northwestern Nebraska, USA. *Palaeontologia Electronica*, **18**(2), 25A, doi:10.26879/508

Böhmer, C., Theil, J. C., Fabre, A. C. & **Herrel, A.** 2020. *Atlas of terrestrial mammal limbs*. CRC Press, Boca Raton, 403 pp.

Brassard, C., Merlin, M., Guintard, C., Monchâtre-Leroy, E., Barrat, J., Bausmayer, N., Bausmayer, S., Bausmayer, A., Beyer, M., Varlet, A., Houssin, C., Callou, C., Cornette, R. & **Herrel, A.** 2020. Bite force and its relationship to jaw shape in domestic dogs. *Journal of Experimental Biology*, **223**, jeb224352.

Bonis, L. D. 1966. Sur l'évolution du genre *Haplocyon* Schlosser (Carnivora). *Bulletin de la Société de France*, **8**, 114–117.

Bowdich, T. E. 1821. *An analysis of the natural classifications of Mammalia, for the use of students and travellers*. J. Smith, Paris, 115 pp.

Calvo, J. P., Pozo, M., Silva, P. G. & **Morales, J.** 2013. Sedimentary infilling of fossil mammal trap formed in pseudokarst at Cerro de los Batallones, Madrid Basin, central Spain. *Sedimentology*, **60**, 1681–1708.

Cerdeño, E & **Sánchez, B.** 1998. *Aceratherium incisivum* (Rhinocerotidae) en el Mioceno superior de Cerro de los Batallones (Madrid). *Revista Española de Paleontología*, **13**, 51–60.

Cohen, K. M., Finney, S. C., Gibbard, P. L. & **Fan, J.-X.** 2013. The ICS International Chronostratigraphic Chart. *Episodes*, **36**, 199–204. Updated at: www. stratigraphy.org/ICSchart/ChronostratChart2018-07

Davis, D. D. 1964 The giant panda — a morphological study of evolutionary mechanisms. *Fieldiana Zoology*, **3**, 1–339.

Domingo, L., Domingo, M. S., Koch, P. L., Morales, J. & **Alberdi, M. T.** 2017. Carnivoran resource and habitat use in the context of a late Miocene faunal turnover episode. *Palaeontology*, **60**, 461–483.

Domingo, M., Alberdi, M. T., Azanza, B. & **Morales, J.** 2012. Mortality patterns and skeletal physical condition of the carnivorans from the Miocene assemblage of Batallones-1 (Madrid Basin, Spain). *Neues Jahrbuch für Geologie und Paläontologie-Abhandlungen*, **265**(2), 131–145.

Domingo, M. S., Alberdi, M. T., Azanza, B., Silva, P. & **Morales, J.** 2013. Origin of an Assemblage Massively Dominated by Carnivorans from the Miocene of Spain. *PLoS ONE*, **8**(5), e63046, doi:10.1371/journal.pone.0063046

Domingo, M. S., Domingo, L., Abella, J., Valenciano, A., Badgley, C. & **Morales, J.** 2016. Feeding ecology and habitat preferences of top predators from two Miocene carnivore-rich assemblages. *Paleobiology*, **42**, 489–507.

Domingo, M. S., Domingo, L., Sánchez, I. M., Alberdi, M. T., Azanza, B. & **Morales, J.** 2011. New insights on the taphonomy of the exceptional mammalian fossil sites of Cerro de los Batallones (Late Miocene; Spain) based on rare earth element geochemistry. *Palaios*, **26**, 55–65.

Domingo, M. S., Cantero, E., García-Real, I., Chamorro Sancho, M. J., Martín Perea, D. M., Alberdi, M. T. & **Morales, J.** 2018. First radiological study of a complete dental ontogeny sequence of an extinct equid: implications for Equidae life history and taphonomy. *Scientific Reports*, **8**, 8507.

Emry, J. R. & **Hunt, R. M. JR.** 1985. Maxillary dentition and new records of *Daphoenicti*s, an Oligocene Amphicyonid carnivore. *Journal of Mammalogy*, **61**,720–723.

Ercoli, M. D., Prevosti, F. J. & **Álvarez, A.** 2012. Form and function within a phylogenetic framework: locomotor habitats of extant predators and some Miocene Sparassodonta (Metatheria). *Zoological Journal of the Linnean Society*, **165**, 224–251.

Ewer, R. F. 1973. *The carnivores*. Cornell University Press, Ithaca, 494 pp.

Fabre, A-C., Salesa, M. J., Cornette, R., Antón, M., Morales, J. & **Peigné, S.** 2015. Quantitative inferences on the locomotor behaviour of extinct species applied to *Simocyon batalleri* (Ailuridae, Late Miocene, Spain*). Science of Nature*, **102**, 30.

Figueirido, B., Pérez−Claros, J. A., Hunt, R. M. JR. & **Palmqvist, P.** 2011. Body mass estimation in amphicyonid carnivoran mammals: a multiple regression approach from the skull and skeleton. *Acta Palaeontologica Polonica*, **56**, 225–246.

Figueirido, B., Pérez−Claros, J. A., Torregrosa, V., Martín−Serra, A. & **Palmqvist, P.** 2010. Demythologizing *Arctodus simus*, the "short−faced" long−legged and predaceous bear that never was. *Journal of Vertebrate Paleontology*, **30**, 262–275.

Ginsburg, L. 1999. Order Carnivora. Pp. 109–148 in G. E. Rössner & K. Heissig (eds) *The Miocene land mammals of Europe*. Friedrich Pfeil, Munich.

Ginsburg, L., Morales, J. & **Soria, D.** 1981. Nuevos datos sobre los carnívoros de los Valles de Fuentidueña (Segovia). *Estudios Geológicos*, **37**, 383–415.

Heizmann, E. P. J. & **Kordikova, E. G.** 2000. Zur systematischen Stellung von "*Amphicyon" intermedius* H. v. Meyer, 1849 (Carnivora, Amphicyonidae). *Carolinea*, **50**, 69–82.

Helbing, H. 1928. Carnivoren des oberen Stampien. *Abhandlungen der Schweizerischen Palaeontologischen Gesellschaft*, **47**, 1–82.

Hocking, D. P., Evans, A. R. & **Fitzgerald, E. M. G.** 2013. Leopard seals (*Hydrurga leptonyx*) use suction and filter feeding when hunting small prey underwater. *Polar Biology*, **36**, 211–222.

Hocking, D. P., Ladds, M. A., Slip, D. J., Fitzgerald, E. M. G. & **Evans, A. R.** 2017. Chew, shake, and tear: Prey processing in Australian sea lions (Neophoca cinerea). *Marine Mammal Science*, **33**, 541–557.

Hough, J. 1948. A systematic revision of *Daphoenus* and some allied genera. *Journal of Paleontology*, **22**, 573–600.

Hunt, R. M. JR. 1974. *Daphoenictis*, a cat-like carnivore (Mammalia, Amphicyonidae) from the Oligocene of North America. *Journal of Paleontology*, **48**, 1030–1047.

Hunt, R. M. JR. 1998. North American Tertiary Amphicyonidae. Pp. 196–227 in C. M. Janis., K. M. Scott & L. L. Jacobs (eds) *Evolution of Tertiary mammals of North America. Volume 1: Terrestrial carnivores, ungulates, and ungulate like mammals*. Cambridge University Press, Cambridge.

Hunt, R. M. JR. 2002. Intercontinental migration of Neogene amphicyonids (Mammalia, Carnivora): appearance of the Eurasian beardog *Ysengrinia* in North America. *American Museum Novitates*, **3384**, 1–53.

Hunt, R. M. JR. 2011. Evolution of large carnivores during the mid-Cenozoic of North America: the temnocyonine radiation (Mammalia, Amphicyonidae). *Bulletin of the American Museum of Natural History*, **358**, 1–153.

Hürzeler, J. 1940a. *Haplocyonoides* nov. gen., ein aberranter Canide aus dem Aquitannien des Hessiers (Mainzer Becken). *Eclogae Geologicae Helv*etiae, **33**, 224–229.

Hürzeler, J. 1940b. Über felinoide Caniden des europäischen Miocäns (Vorläufige Mitteilung). *Eclogae Geologicae Helv*etiae, **33**, 229–230.

Janis, C. M., Figueirido, B., Desantis, L. & **Lautenschlager, S.** 2020. An eye for a tooth: *Thylacosmilus* was not a marsupial "saber-tooth predator". *PeerJ*, **8**, e9346, doi:10.7717/peerj.9346

Kohno, N. 1997. The first record of an amphicyonid (Mammalia: Carnivora) from Japan, and its implication for amphicyonid paleobiogeography. *Paleontological Research*, **1**, 311–315.

Kaup, J. 1832. Vier neue Arten urweltlicher Raubthiere welche im zoologischen Museum zu Darmstadt aufbewart werden. *Archives für Mineralogie*, **5**, 150–158.

Kaup, J. 1833. *Description d'ossements fossiles de Mammifères inconnus jusqu'à présent qui se trouvent au Muséum grand-ducal de Darmstadt*. Darmstadt J. G., Heyer, 119 pp.

Kretzoi, M. 1943. *Kochictis centennii* n. g. n. sp. az egeresi felső oligocénől. *Földtani Közlöny*, **73**, 10–17.

Kuss, S. E. 1962. Problematische Caniden des europaïschen Tertiärs. *Berichte der Naturforschenden Gesellschaft Freiburg im Breisgau*, **32**, 123–172.

Kuss, S. E. 1965. Revision der Europaschen Amphicyoninae (Canidae, Carnivora, Mammalia) ausschliesslich der voroberstampischen Formen. *Sitzungsberichte der Heidelberger Akademie der Wissenschaften Mathematisch-naturwissenchaftliche Klasse*, **1**, 1–168.

López-Antoñanzas, R., Peláez-Campomanes, P., Álvarez-Sierra, M. A. & **García Paredes, I.** 2010 New species of *Hispanomys* (Rodentia, Cricetodontinae) from the Upper Miocene of Batallones (Madrid, Spain). *Zoological Journal of the Linnean Society*, **160**, 725–747.

López-Antoñanzas, R., Peláez-Campomanes, P. & **Álvarez-Sierra, M. A.** 2014 New Species of *Rotundomys* (Cricetinae) from the Late Miocene of Spain and Its Bearing on the Phylogeny of *Cricetulodon* and *Rotundomys*. *PLoS ONE*, **9**(11), e112704, doi:10.1371/journal.pone.0112704

Martín-Perea, D. M., Courtenay, L. A., Domingo, M. S. & **Morales, J.** 2020. Application of artificially intelligent systems for the identification of discrete fossiliferous levels. *PeerJ*, **8**, e8767, doi:10.7717/peerj.8767

Mayet, L. 1908. Études de Mammifères miocènes des sables de l'Orléanais et des faluns de la Touraine. *Annales de l'Université de Lyon, nouvelle série*, **24**, 1–336.

Medina-Chavarrías, V., Oliver, A., López-Guerrero, P., Peláez-Campomanes, P. & **Álvarez-Sierra, M. A.** 2019. New insights on *Hispanomys moralesi* (Rodentia, Mammalia) and its use as biostratigraphical indicator. *Journal of Iberian Geology*, **45**, 641–654.

Mein, P. & **Ginsburg, L.** 2002. Sur l'âge relatif des différents dépôts karstiques Miocènes de La Grive-Saint-Alban (Isère). *Cahiers scientifiques-Muséum d'Histoire naturelle, Lyon*, **2**, 7–47.

Meyer, H. Von 1849. Letter on various fossils. *Neues Jahrbuch für Geologie und Paläontologie*, **1849**, 547–550.

Monescillo, M. N. F., Salesa, M. J., Antón, M., Siliceo, G. & **Morales, J.** 2014. *Machairodus aphanistus* (Felidae, Machairodontinae, Homotherini) from the late Miocene (Vallesian, MN 10) site of Batallones-3 (Torrejón de Velasco, Madrid, Spain). *Journal of Vertebrate Paleontology*, **34**, 699–709.

Morales J. 2017. Vertebrados miocenos de los yacimientos del Cerro de los Batallones. Pp. 36–40 in J. Morales (ed.) *La colina de los Tigres Dientes de sable. Los yacimientos miocenos del Cerro de los Batallones (Torrejón de Velasco, Comunidad de Madrid)*. Museo Arqueológico Regional, Comunidad de Madrid, Alcalá de Henares.

Morales, J., Pickford, M. & **Valenciano, A.** 2016. Systematics of African Amphicyonidae, with descriptions of new material from Napak (Uganda) and Grillental (Namibia). *Journal of Iberian Geology*, **42**, 131–150.

Morales J., Abella J. & **Valenciano A.** 2017. *Thaumastocyon*: los extraños Amphicyonidae de Batallones 3. Pp. 338–351 in J. Morales (ed.) *La colina de los Tigres Dientes de sable. Los yacimientos miocenos del Cerro de los Batallones (Torrejón de Velasco, Comunidad de Madrid)*. Museo Arqueológico Regional, Comunidad de Madrid, Alcalá de Henares.

Morales, J., Fejfar, O., Heizmann, E., Wagner, J., Valenciano, A. & **Abella, J.** 2019. A new Thaumastocyoninae (Amphicyonidae, Carnivora) from the early Miocene of Tuchořice Czech Republic. *Fossil Imprint*, **75**, 397–411.

Morlo, M., Bastl, K., Habersetzer, J., Engel, T., Lischewsky, B., Lutz, H., Von Berg, A., Rabenstein, R. & **Nagel, D.** 2020. The apex of amphicyonid hypercarnivory: solving the riddle of *Agnotherium antiquum* Kaup, 1833 (Mammalia, Carnivora). *Journal of Vertebrate Paleontology*, **39**, e1705848.

Noulet J. B. 1876. Note sur un gisement du *Canis palaeolycos*, dans le Miocène toulousain. *Mémoires de l'Académie des Sciences, Inscriptions et Belles-Lettres de Toulouse*, **8**, 400–403.

Peigné, S. & **Heizmann, E. P. J.** 2003. The Amphicyonidae (Mammalia: Carnivora) from the Early Miocene locality of Ulm-Westtangente, Baden-Württemberg, Germany: systematics and ecomorphology. *Stuttgarter Beiträge zur Naturkunde, Serie B (Geologie und Paläontologie)*, **343**, 1–133.

Peigné, S., Salesa, M. J., Antón, M. & **Morales, J.** 2005. Ailurid carnivoran mammal *Simocyon* from the late Miocene of Spain and the systematics of the genus. *Acta Paleontologica Polonica*, **50**, 219–238.

Peigné, S., Salesa, M. J., Antón, M. & **Morales, J.** 2008. A new Amphicyonine (Carnivora: Amphicyonidae) from the Upper Miocene of Batallones-1, Madrid, Spain. *Palaeontology*, **51**, 943–965.

Peterson, O. A. 1907. The Miocene beds of western Nebraska and eastern Wyoming and their vertebrate faunae. *Annals of the Carnegie Museum*, **4**, 21–72.

Pérez-García, A. & **Murelaga, X.** 2013. Las tortugas del Vallesiense superior del Cerro de los Batallones (Madrid, España): Nuevos datos sobre el escasamente conocido geénero Paleotestudo. *Ameghiniana*, **50**, 335–353.

Pérez-García, A. & **Vlachos, E.** 2014. New generic proposal for the European Neogene large testudinids (Cryptodira) and the first phylogenetic hypothesis for the medium and large representatives of the European Cenozoic record. *Zoological Journal of the Linnean Society*, **172**, 653–719.

Pickford, M. 2015. Late Miocene Suidae from Eurasia: the *Hippopotamodon* and *Microstonyx* problem revisited. *Münchner Geowissenschaftliche Abhandlungen*, **42**, 1–124.

Pomel, A. 1846. Mémoire pour servir à la géologie paléontologique des terrains tertiaires du département de l´Allier. *Bulletin de la Société géologique de France,* **3**, 353–373.

Qiu, Z.-D. & **Qiu, Z.-X.** 2013. Chapter 4. Early Miocene Xiejiahe and Sihong Fossil localities and their faunas, Eastern China. Pp. 142–154 in X. Wang, L. J. Flynn & M. Fortelius (eds) *Fossil mammals of Asia. Neogene biostratigraphy and chronology.* Columbia University Press, New York.

Qiu, Z.-X., Yan, D.-F., Jia, H. & **Sun, B.** 1986. The large-sized Ursid fossil from Shanwang, Shandong. *Vertebrata PalAsiatica*, **24**, 182–194.

Riggs, E. S. 1934. A new marsupial sabertooth from the Pliocene of Argentina and its relationships to other South American predaceous marsupials. *Transactions of the American Philosophical Society*, **24**, 1–32.

Ríos, M. & **Morales, J.** 2019. A new skull of *Decennatherium rex* Ríos, Sánchez and Morales, 2017 from Batallones-4 (upper Vallesian, MN10, Madrid, Spain). *Palaeontologia Electronica*, 22.2.pvc_1, 1–16, doi:10.26879/965

Ríos, M., Sánchez, I. M. & **Morales, J.** 2017. A new giraffid (Mammalia, Ruminantia, Pecora) from the late Miocene of Spain, and the evolution of the sivathere-samothere lineage. *PLoS ONE*, **12**(11), e0185378, doi:10.1371/journal.pone.0185378

Robles, J. M., Alba, D. M., Fortuny, J., De Esteban-Trivigno, S., Rotgers, C., Balaguer, J., Carmona, R., Galindo, J., Almécija, S., Bertó, J. V. & **Moyà-Solà, S.** 2013. New craniodental remains of the barbourofelid Albanosmilus jourdani (Filhol, 1883) from the Miocene of the Vallès-Penedès Basin (NE Iberian Peninsula) and the phylogeny of the Barbourofelini. *Journal of Systematic Palaeontology*, **11**, 993–1022.

Salesa, M. J., Antón, M., Morales, J. & **Peigné, S.** 2012 Systematics and phylogeny of the small felines (Carnivora, Felidae) from the Late Miocene of Europe: a new species of Felinae from the Vallesian of Batallones (MN 10, Madrid, Spain). *Journal of Systematic Palaeontology*, **10**, 87–102.

Salesa, M. J., Antón, M., Turner, A. & **Morales, J.** 2005. Aspects of the functional morphology in the cranial and cervical skeleton of the sabretoothed cat *Paramachairodus ogygia* (Kaup, 1832) (Felidae, Machairodontina) from the Late Miocene of Spain: Implications for the origins of the machairodont killing bite. *Zoological Journal of the Linnean Society*, **144**, 363–377.

Salesa, M. J., Antón, M., Turner, A. & **Morales, J.** 2006. Inferred behaviour and ecology of the primitive sabre-toothed cat *Paramachairodus ogygia* (Felidae machairodontinae) from the Late Miocene of Spain. *Journal of Zoology*, **268**, 243–254.

Salesa, M. J., Antón, M, Turner, A. & **Morales, J.** 2010. Functional anatomy of the forelimb in *Promegantereon* ogygia* (Felidae, Machairodontinae, Smilodontini) from

the Late Miocene of Spain and the origins of the sabre-toothed felid model. *Journal of Anatomy*, **216**, 381–396.

Salesa, M. J., Siliceo, G., Antón, M., Peigné, S. & **Morales, J.** 2019. Functional and systematic implications of the postcranial anatomy of a Late Miocene feline (Carnivora, Felidae) from Batallones-1 (Madrid, Spain). *Journal of Mammalian Evolution*, **26**, 101–131.

Sánchez, I. M., Quiralte, V. & **Morales, J.** 2011. Presence of the bovid *Austroportax* in the upper Miocene fossil site of Batallones-1 (MN10, Madrid Basin, Spain). *Estudios Geológicos*, **67**, 637–642.

Sánchez, I. M., Domingo, S. & **Morales, J.** 2009. New data on the Moschidae (Mammalia, Ruminantia) from the Upper Miocene of Spain (MN10- MN11). *Journal of Vertebrate Paleontology*, **29**, 567–575.

Schaller, O. 2007. *Illustrated veterinary anatomical nomenclatures*. Second edition. Enke Verlag, Stuttgart, 614 pp.

Siliceo, G. 2015. *Anatomía funcional y paleobiología de* Magericyon anceps *(Amphicyonidae, Carnivora) del complejo de yacimientos vallesienses (Mioceno superior, MN 10) del Cerro de los Batallones (Torrejón de Velasco, Madrid)*. Unpublished PhD thesis, Universidad de Alcalá, 360 pp.

Siliceo, G., Antón, M., Morales, J. & **Salesa, M. J.** 2019. Built for strength: functional insights from the thoracolumbar and sacrocaudal regions of the late Miocene amphicyonid *Magericyon anceps* (Carnivora, Amphicyonidae) from Batallones-1 (Madrid, Spain). *Journal of Mammalian Evolution*, **26**, 101–131.

Siliceo, G., Salesa, M. J., Antón, M., Monescillo, M. N. F. & **Morales, J.** 2014. *Promegantereon ogygia* (Felidae, Machairodontinae, Smilodontini) from the Vallesian

(late Miocene, MN 10) of Spain: morphological and functional differences in two noncontemporary populations. *Journal of Vertebrate Paleontology*, **34**, 407–418.

Siliceo, G., Salesa, M. J., Antón, M., Pastor, J-F. & **Morales, J.** 2015. Comparative anatomy of the shoulder region in the late Miocene amphicyonid *Magericyon anceps* (Carnivora): functional and paleoecological inferences. *Journal of Mammalian Evolution*, **22**, 243–258.

Siliceo, G., Salesa, M. J., Antón, M., Peigné, S. & **Morales, J.** 2017. Functional anatomy of the cervical region in the late Miocene amphicyonid *Magericyon anceps* (Carnivora, Amphicyonidae): implications for its feeding behaviour. *Palaeontology*, **60**(3), 1–19.

Springhorn, R. 1997. Revision der Alttertiären Europäischen Amphicyonidae (Carnivora, Mammalia). *Palaeontographica (A)*, **158**, 26–113.

Stehlin, H. G. & **Helbing, H.** l925. Catalogue des Ossesments de Mammifères Tertiaires de Ia Collection Bourgeois. *Bulletin de la Société d'Histoire Naturelle et d'Anthropologie du Loir-et-Cher*, **18**, 77–277.

Swofford, D. L. 2002. PAUP*. *Phylogenetic Analysis using Parsimony (*and other methods).* Version 4. Sinauer Associates, Sunderland, Massachusetts.

Therrien, F. 2005. Mandibular force profiles of extant carnivorans and implications for the feeding behaviour of extinct predators. *Journal of Zoology*, **267**, 249–270.

Trouessart, E. 1885. Catalogue des mammifères vivants et fossiles. Carnivores. *Bulletin de la Société des Études Scientifiques, Angers*, **14**[supplement to the year 1884], 1–108.

Tseng, Z-J., Takeuchi, G. T. & **Wang, X.** 2010. Discovery of the upper dentition of *Barbourofelis whitfordi* (Nimravidae, Carnivora) and an evaluation of the genus in California, *Journal of Vertebrate Paleontology*, **30**, 244–254.

Valenciano, A., Abella, J., Sanisidro, O., Hartstone-Rose, A., Álvarez Sierra, M. A. & **Morales, J.** 2015. Complete description of the skull and mandible of the giant mustelid

Eomellivora piveteaui Ozansoy, 1965 (Mammalia, Carnivora, Mustelidae), from Batallones (MN10), late Miocene (Madrid, Spain). *Journal of Vertebrate Paleontology*, **35**(4), e934570.

Valenciano, A., Pérez-Ramos, A., Abella, J. & **Morales, J.** 2020. A new hypercarnivorous mustelid (Mammalia, Carnivora, Mustelidae) from Batallones, late Miocene (MN10), Torrejón de Velasco, Madrid, Spain. *Geodiversitas*, **42**(8), 103–121.

Villa, A., Abella, J., Alba, D. M., Almécija, S., Bolet, A., Koufos, G. D., Knoll, F., Luján, A. H., Morales, J., Robles, J. M., Sánchez I. M. & **Delfino, M.** 2018. Revision of *Varanus marathonensis* (Squamata, Varanidae) based on historical and new material: morphology, systematics, and paleobiogeography of the European monitor lizards. *PLoS ONE*, **13**(12), e0207719, doi:10.1371/journal.pone.0207719

Viranta, S. 1996. European Miocene Amphicyonidae – taxonomy, systematics and ecology. *Acta Zoologica Fennica*, **204**, 1–61.

Viret, J. 1929a. Les faunes de Mammifères de l'Oligocène supérieur de la Limagne bourbonnaise. *Annales de l'Université de Lyon, nouvelle série 1*, **47**, 1–329.

Viret, J. 1929b. *Tomocyon grivensis* et les Canidés de La Grive-Saint-Alban. *Bulletin de la Société géologique de France*, **29**, 217–226.

Wang, X. M., Wang, H. J. & **Jiangzuo, Q. G.** 2016. New record of a haplocyonine amphicyonid in early Miocene of Nei Mongol fills a long-suspected geographic hiatus. *Vertebrata PalAsiatica*, **54**, 21–35.

Werdelin, L. & **Peigné, S.** 2010. Carnivora. Pp. 603–657 in L. Werdelin & W. Sanders (eds) *Cenozoic mammals of Africa*. University of California Press, Los Angeles:

Werdelin L. & **Simpson S. W.** 2009. The last amphicyonid (Mammalia, Carnivora) in Africa. *Geodiversitas*, **31**(4), 775–787.

Wortman, J. L. 1901. A new American species of *Amphicyon*. *American Journal of Science*, **11**, 200–204.

Figure captions

Figure 1. A, map of the Iberian Peninsula showing the location of Madrid and Valdemoro. **B,** location of Batallones-3 sites, west of Valdemoro.

Figure 2. *Ammitocyon kainos* gen. et sp. nov. from Batallones-3, Spain. **A, B, C, D, E, F, G,** BAT-3'10.1689, skull (paratype). **A,** dorsal view; **B,** ventral view (stereo pair); **C**, lateral view; **D,** caudal view; **E,** rostral view; **F,** right P4–M2 in occlusal view; **G,** left P4–M1 in occlusal view.

Figure 3. *Ammitocyon kainos* gen. et sp. nov. from Batallones-3, Spain. A, B, J, BAT-3'11.453, mandible (paratype). **A,** buccal view; **B,** occlusal view; **J,** rostral view; C,E, G BAT-3'09.1239, right hemimandible (holotype). **C,** buccal view; **E,** occlusal view; **G,** lingual view; D, F, H, BAT-3'08.604 left hemimandible (holotype). **D,** buccal view; **F,** occlusal view; **H,** lingual view; **I,** BAT-3'09.1239 and BAT-3'08.604, rostral composition view of the two hemimandibles.

Figure 4. *Ammitocyon kainos* gen. et sp. nov. from Batallones-3, Spain. A, C, E, BAT-3'09.1239, postcanine right lower dentition (holotype). **A,** lingual view; **C,** occlusal

view; **E,** buccal view; B, D, F, BAT-3'09.1124, isolated left m2 (paratype). **B,** buccal view; **D,** occlusal view; **F,** lingual view (stereo images).

Figure 5. Skeletal reconstruction of *Ammitocyon kainos* gen. et sp. nov. from Batallones-3, Spain. Photographs used for recovered fossils of *A. kainos* from BAT-3; idealized skeleton in 3D images reconstructed for the rest of the skeleton. Measurements of scapula and long bones in Supplemental file 6.

Figure 6. Phylogenetic relationship of *Ammitocyon kainos* gen. et sp. nov. (majority rule tree), within some selected Amphicyonidae. *Pseudocyonopsis landesquei* is the outgroup. Searches were performed by means of the Branch and Bound and a bootstrap analysis through 1,000 replicates. Eight trees are obtained (length 102 steps, consistency index (CI) = 0.6373, homoplasy index (HI) = 0.3627, retention index (RI) = 0.6891). Clade support was calculated using bootstrap analysis with 1,000 replicates, and Bremer support values. The numbers below nodes are Bremer indices, and the numbers above nodes are Bootstrap support percent-ages (only shown ≥ 50)

Figure 7. Biochronology and hypothesis of phylogenetic relationships of the species of Thaumastocyoninae and selected Amphicyoninae based on the obtained tree (Fig. 6). Chronological data after Cohen *et al*. (2013). Temporal range of the species based on Hunt (1998); Ginsburg (1999); Peigné & Heizmann (2003); Morales *et al.* (2019). **Specimens figured**: ***Daphoenodon superbus*** Peterson (1910) CM 1589 cast of the holotype Skull from Agate Fossil Beds National Monument, USA. ***Ysengrinia americana*** (Wortman, 1901) YPM 10061 cast of the holotype palate, original from Harrison Formatio, USA (see Hunt, 2002). ***Crassidia intermedia*** (von Meyer, 1849)

SMNS 4568 right M1 figured by Heizmann & Kordikova (2000) from Ulm, Germany (mirrored). ***Ysengrinia gerandiana*** (Viret 1929a) MNHN-SG 393 reconstructed left and right M1 from Saint Gérand le Puy, France. ***Peignecyon felinoides*** Morales *et al.* (2019) TU 73916 right M1 from Tuchořice, the Czech Republic (mirrored). ***Ysengrinia valentiana*** Belinchon & Morales (1989) PaN 319 left M1 from Buñol, Spain. ***Thaumastocyon bourgeoisi*** Sthelin & Helbing (1925) Pont Levoy 705 left M1from Pont Levoy, France ***Thaumastocyon dirus*** Ginsburg *et al.* (1991) LVF-6 right M1 from Los Valles de Fuentidueña, Spain (mirrored). ***Ammitocyon kainos*** BAT-3'10.1689 reconstructed skull post canine dentition P4–M2, (P4–M1 left side, M2 right side) from Batallones-3, Spain. ***Tomocyon grivensis*** Viret (1929b) LGR-1121 left M1 from La Grive Saint Alban, France.

Figure 8. Mandibular force profiles of *Ammitocyon kainos*, *Panthera leo*, *Crocuta crocuta* and *Canis lupus*. Values are presented for canine, p3–p4, p4–m1, m1–m2 and post-m2 interdental gaps (when possible). Darker line represents values for each species and grey lines the values of the other species used for comparison.

Figure 9. *Ammitocyon kainos* gen. et sp. nov. from Batallones-3, Spain. **A,** skull and cervical vertebrae. (Idealized). **B,** reconstructed life appearance of the head and neck (drawing by Oscar Sanisidro).

Table captions

Table 1. Measurements (in mm) of the dentition of *Ammitocyon kainos* gen. et sp. nov. from Batallones-3, Spain. **Abbreviations: L**, length; **H**, height; **W**, width.

Table 2. Measurements of cranium and mandible of *Ammitocyon kainos* gen. et sp. nov. from Batallones-3, Spain. **Abbreviations: lbC**, basal length of the skull, from the rostral part of the premaxilla to the rostral edge of the foramen magnum; **lMM**, maximum mandibular length, from the central point of the mandibular condyle to the most rostral end; **Hc**, height of the mandibular body at the level of the canine; **Hm**, maximum mandibular height; **lc**, length of the mandibular body from the condyle to the mesial border of the canine; **Hp4m1**, height of the mandibular body at the level of the interdental space between p4 and m1; **lp4m1**, length of the mandibular body from the central point of the condyle to the interdental space between p4 and m1.

Table 3. Mandibular force profiles of *Panthera leo*, *Crocuta crocuta*, *Canis lupus*, *Borocyon robustum*, *Delotrochanter oryktes*, *Temnocyon macrogenys*, *Magericyon anceps* and *Ammitocyon kainos*. Log Zx/L represents dorsoventral force resistance; Log Zy/L represents labiolingual force resistance; Zx/Zy represents relative values for force resistance. Values for *P. leo*, *C. crocuta*, *Ca. lupus*, *B. robustum*, *D. oryktes*, *T. macrogenys* from Therrien (2005) and Hunt (2011). Values for *M. anceps* and *A. kainos* measured for this work.

Supplemental file captions

Supplemental file 1. Complete list of 54 equally weighted and unordered cranial, mandibular, and dental characters used in the cladistic analysis.

Supplemental file 2. Character-taxon matrix (13 taxa and 54 characters) in nexus format used in the cladistic analysis.

Supplemental file 3. Synapomorphies for selected nodes (see Figure 6), as indicated by character numbers followed by character states within parentheses. Italics denote ambiguous synapomorphies.

Supplemental file 4. A. Stereophotograhs of the skull of *Ammitocyon kainos* (BAT-3'10.1689, skull paratype) in dorsal view. B. Stereophotograhs of the skull of *Magericyon anceps* (BAT-3'13.2000) in dorsal view.

Supplemental file 5. Basicranium of *Ammitocyon kainos* (BAT-3'10.1689, skull paratype) in ventral view. Abbreviations: gf: glenoid fossa; fo: foramen ovale; pf: postglenoid foramen; ab: auditory bulla; sf: stylomastoid foramen; pp: paraoccipital process; oc: occipital condyles; plf: posterior lacerate foramen; mp: mastoid process.

Supplemental file 6. Measurements (in mm) of the scapula, stylopod and zeugopod bones of *Ammitocyon kainos* from Batallones-3, found associated to the skull BAT-3’10.1689.

A= proximal-distal maximum length; B= cranial-caudal proximal epiphysis width; C=medial-lateral proximal epiphysis width; D=cranial-caudal mid-diaphysis width;

E=medial-lateral mid-diaphysis width; F= cranial-caudal distal epiphysis width; G=medial-lateral distal epiphysis width.

In the scapula, measurements of B and C were taken at the glenoid cavity, and G of the maximum width of the medial border. In the ulna measurements B and C were taken at the olecranon above the trochlear notch.

Specimen	LC	WC	HC	LP4	WP4	LM1	WM1	LM2	WM2
BAT-3'10 1689 left	26.0	16.0	43.0	35.3	18.9	16.9	20.8		
BAT-3'10 1689 right	27.5	16.0	40.0	36.9	18.5	16.6	20.1	12.6	14.5

Specimen	Lc	Wc	Hc	Lp4	Wp4	Lm1	Wm1	Lm2	Wm2
BAT-3'11 453 right	30.0	16.0	36.5						
BAT-3'09 1239	24.0			20.15	9.2	29.7	13.2	18.0	9.4
BAT-3'08 604	24.0	16.0	42.0	20.2	8.5	28.6	12.3	15.4	7.9
BAT-3'09 1124								15.2	8.9

Specimen	BAT-3'10 1689	BAT-3'08 604	BAT-3'09 1239	BAT-3'11 453 Left	BAT-3'11 453 Right
lbC	379.59				
lMM			233.7	252.2	253.7
lc			223.55	243.8	251.85
Hc		55.07	50.03	47.7	53.1
Hp4m1		53.85	51.23	55,63	47.42
lp4m1			137.06	142.15	149.2
Hm		128.06	125.26		

Log Zx/L						
	post m3	post m2	m1-m2	p4-m1	p3-p4	Canine
Panthera leo			-0.29	-0.47	-0.64	-0.38
Crocuta cocuta			-0.23	-0.45	-0.67	-0.61
Canis lupus	-0.47	-0.55	-0.64	-0.77	-0.97	-0.92
Borocyon robustum	-0.07	-0.21	-0.31	-0.54	-0.67	-0.55
Delotrochanter oryktes	-0.28	-0.34	-0.49	-0.73	-0.85	-0.55
Temnocyon macrogenys	-0.19	-0.26	-0.46	-0.65	-0.8	-0.58
Magericyon anceps		-0.92	-1.00	-1.27	-1.40	-0.60
Ammitocyon kainos		-0.99	-1.17	-1.13	-1.38	-0.78

Log Zy/L						
	post m3	post m2	m1-m2	p4-m1	p3-p4	Canine
Panthera leo			-0.64	-0.80	-0.93	-0.48
Crocuta cocuta			-0.76	-0.83	-0.96	-0.69
Canis lupus	-0.98	-1.05	-1.07	-1.09	-1.26	-0.88
Borocyon robustum	-0.59	-0.67	-0.71	-0.93	-1.02	-0.63
Delotrochanter oryktes	-0.94	-0.94	-1.00	-1.16	-1.34	-0.71
Temnocyon macrogenys	-0.83	-0.89	-1.05	-1.07	-1.3	-0.69
Magericyon anceps		-0.41	-0.51	-0.79	-0.92	-0.52
Ammitocyon kainos		-0.32	-0.47	-0.58	-0.76	-0.22

Zx/Zy						
	post m3	post m2	m1-m2	p4-m1	p3-p4	Canine
Panthera leo			2.28	2.11	1.94	1.25
Crocuta cocuta			3.43	2.37	1.93	1.20
Canis lupus	3.23	3.10	2.67	2.12	1.94	0.90
Borocyon robustum	3.33	2.88	2.56	2.41	2.23	1.2
Delotrochanter oryktes	4.51	4.01	3.24	2.67	3.13	1.46
Temnocyon macrogenys	4.35	4.05	3.73	2.66	3.23	1.3
Magericyon anceps		0.31	0.33	0.33	0.33	0.83
Ammitocyon kainos		0.21	0.20	0.28	0.24	0.27

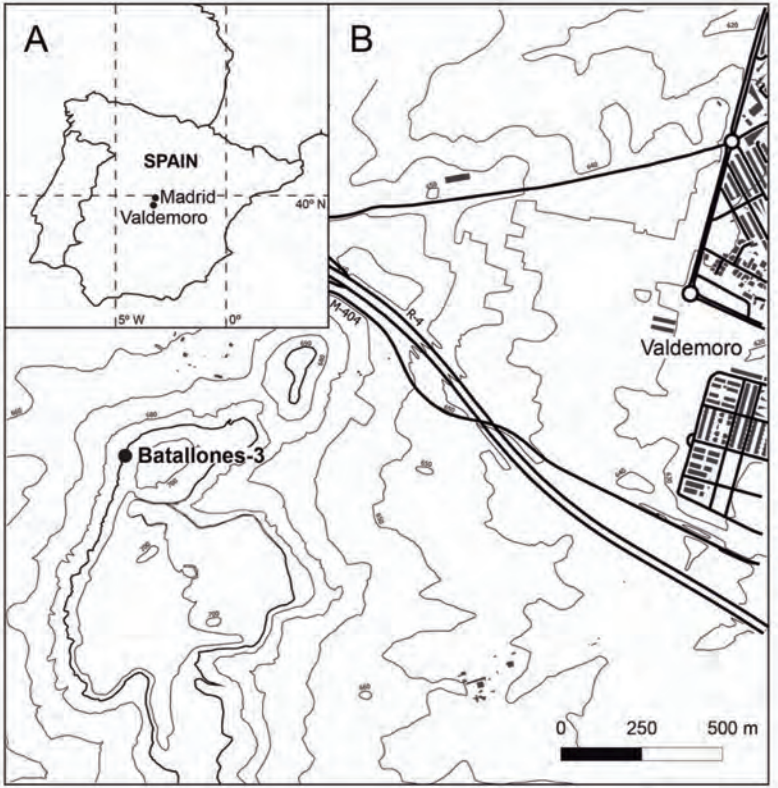
A
SPAIN
Madrid
Valdemoro
40º N
5º W
0º
B
M-404
R-4
Valdemoro
Batallones-3
0
250
500 m

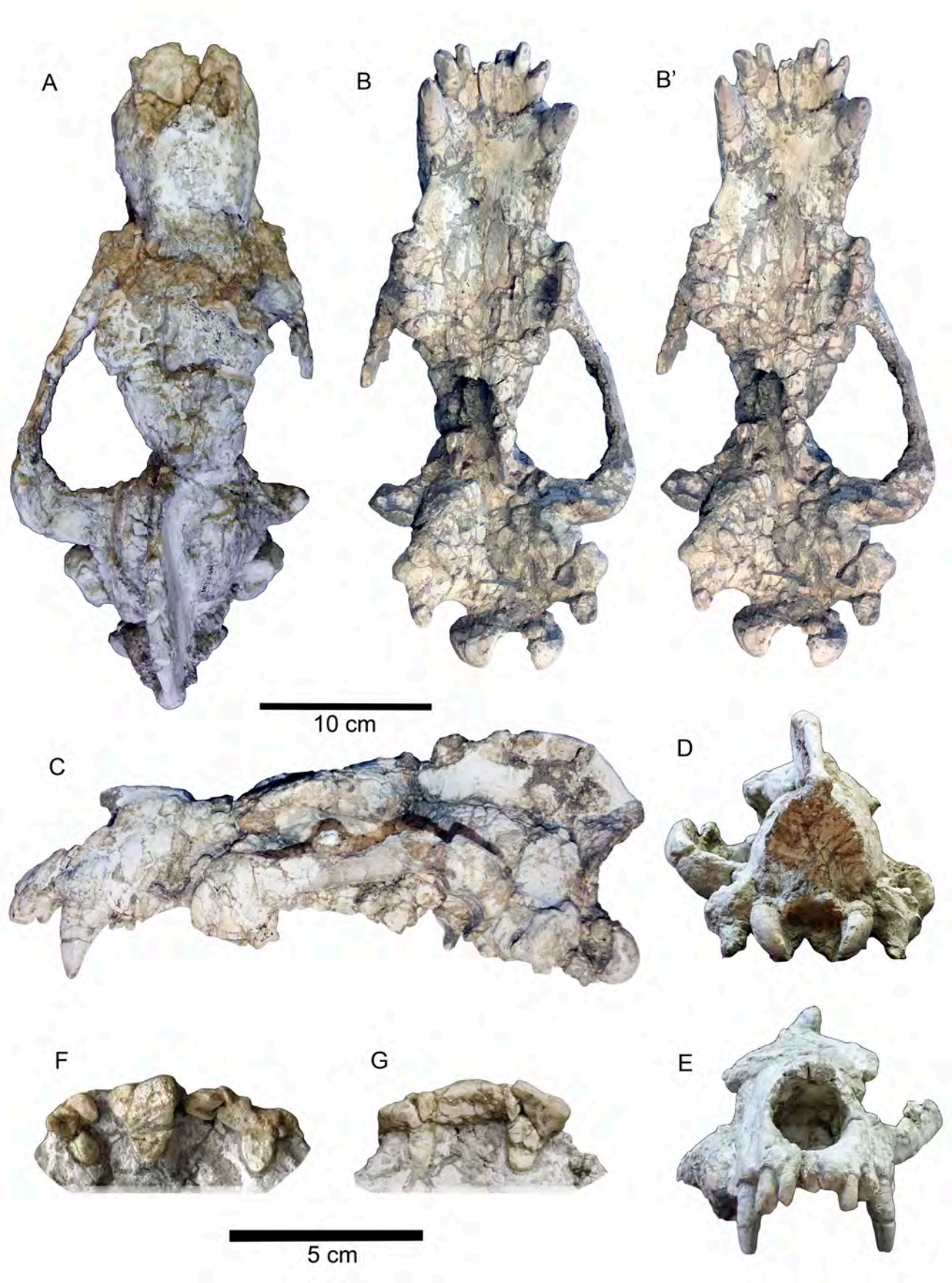
A
B
B'
10 cm
C
D
F
G
E
5 cm

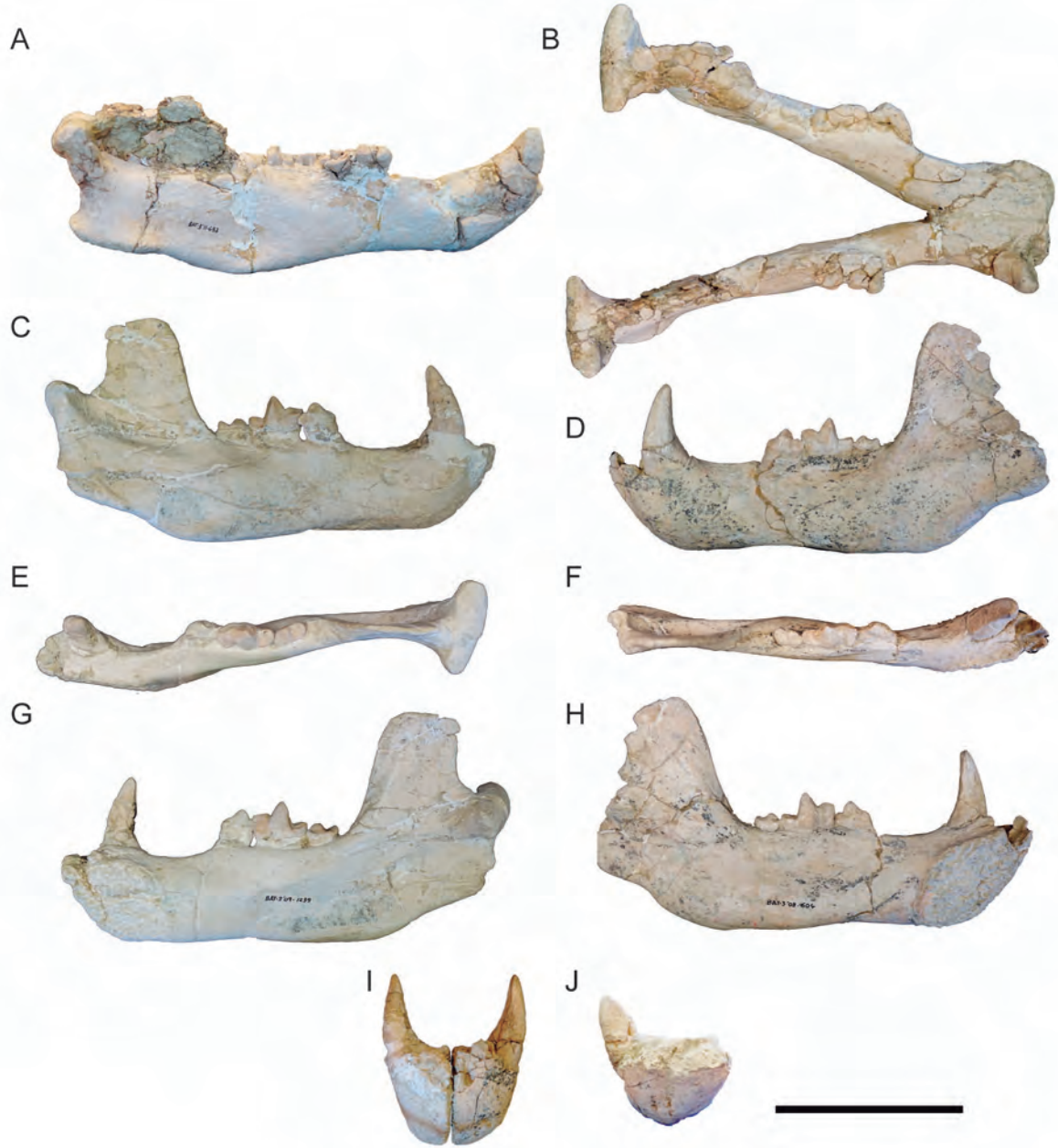
A
B
C
D
E
F
G
H
I
J

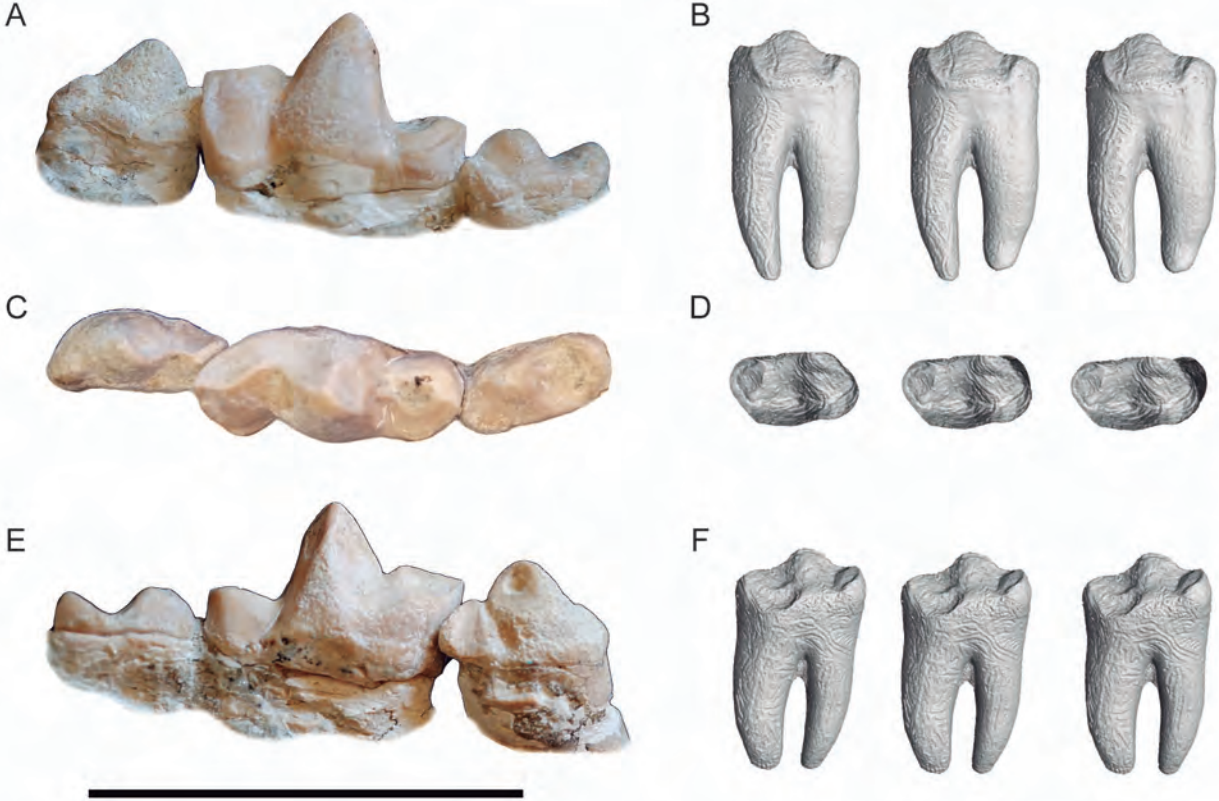
A
B
C
D
E
F

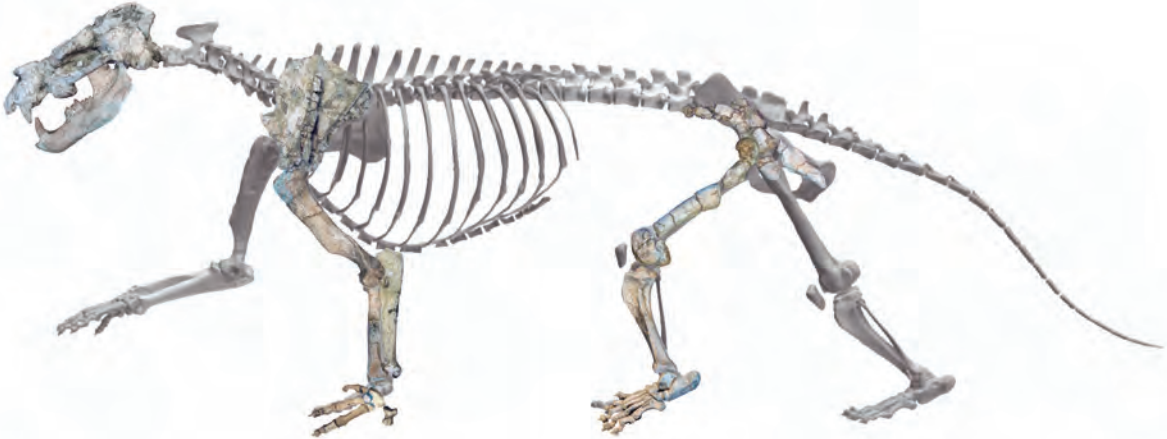

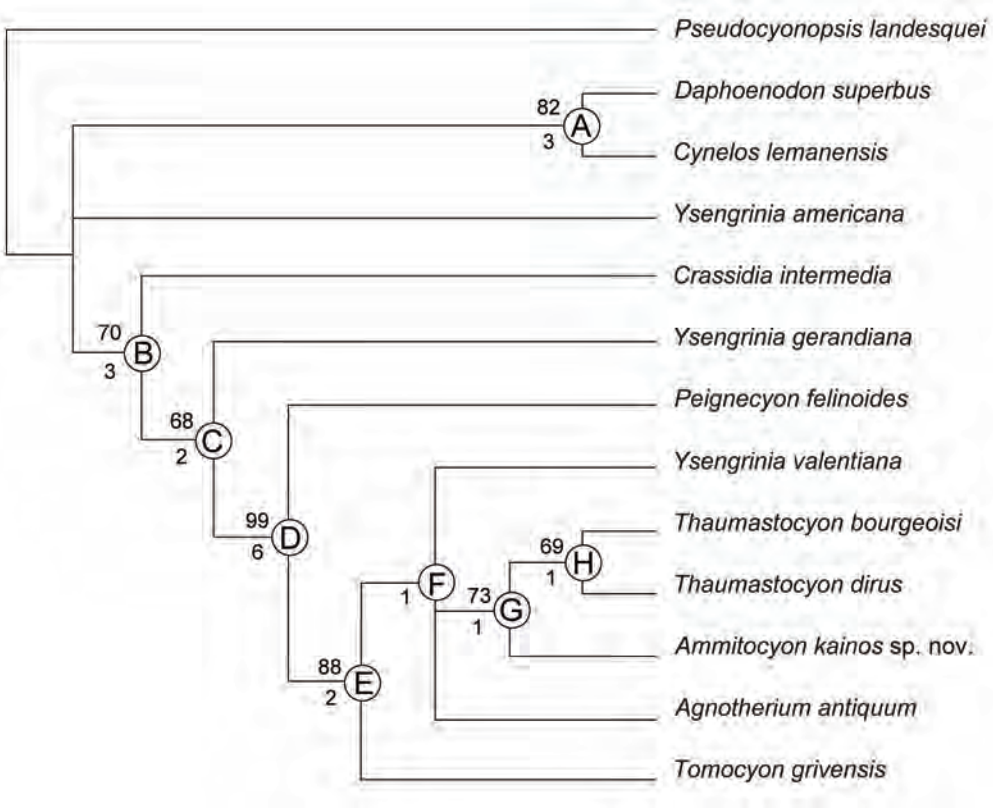
Pseudocyonopsis landesquei
Daphoenodon superbus
Cynelos lemanensis
Ysengrinia americana
Crassidia intermedia
Ysengrinia gerandiana
Peignecyon felinoides
Ysengrinia valentiana
Thaumastocyon bourgeoisi
Thaumastocyon dirus
Ammitocyon kainos sp. nov.
Agnotherium antiquum
Tomocyon grivensis
A
82
3
B
70
3
C
68
2
D
99
6
E
88
2
F
1
G
73
1
H
69
1

Epoch
Stage
Miocene
Late
Middle
Early
Oligocene
Late
Early
Eocene
Messinian
Tortonian
Serravallian
Langhian
Burdigalian
Aquitanian
Chattian
Rupelian
10
15
20
25
30
35
Pseudocyonopsis landesquei
Daphoenodon superbus
Cynelos lemanensis
Ysengrinia americana
Crassidia intermedia
Ysengrinia gerandiana
Peignecyon felinoides
Ysengrinia valentiana
Thaumastocyon bourgeoisi
Thaumastocyon dirus
Ammitocyon kainos
Agnotherium antiquus
Tomocyon grivensis
1

(figures not to scale)

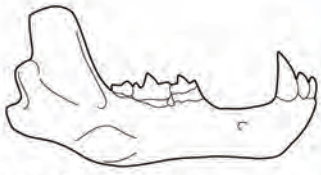

Ammitocyon kainos
(L= 25.4 cm; average)

Panthera leo (L= 22.95 cm)

Crocuta crocuta (L= 17.50 cm)

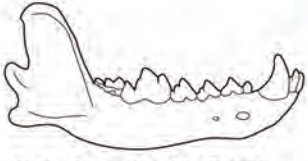

Canis lupus (L= 19.13 cm)

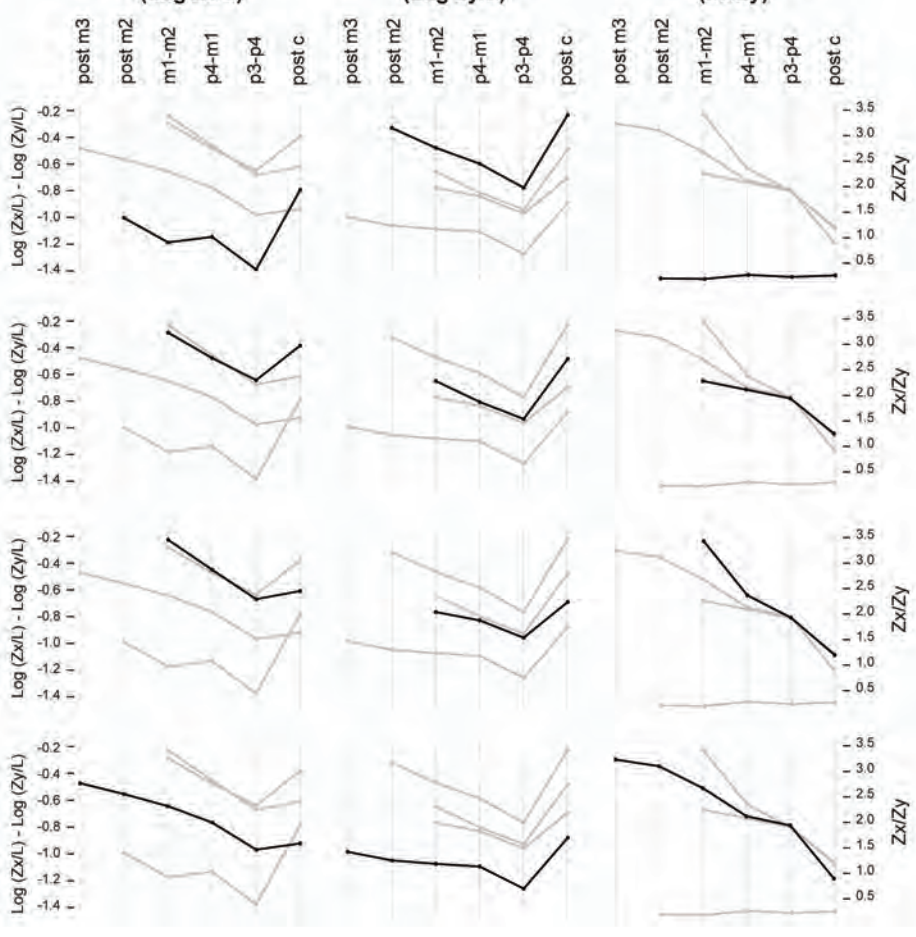


A
B